by HSA-DB-L treatment ($P>0.05$). Furthermore, the plasma level of CPT in HSA-DB-L-treated mice remained 60-fold higher than that in mice treated with CPT solution.

4. Discussion

Stable pegylated liposome-incorporated CPT was obtained by the addition of DB to the formulation for liposomes combined with coating the surface of the liposomes with HSA. The CPT liposomes showed activity against C26 tumors resulting from high accumulation of CPT in the tumors when administered as a single i.v. injection in mice.

To improve the pharmacological usefulness of CPT, a liposomal formulation including CPT was developed, and the CPT liposomes were evaluated regarding their particle size, incorporation efficiency, drug release in vitro, and stability in vivo. Liposomes composed of HSPC and Ch showed low retention in the blood 4 h after injection (0.09% of injected dose of CPT). Addition of OA to the liposomes increased the retention of the injected dose of CPT to 0.4% (data not shown), suggesting that OA might increase the acidity of liposomes, resulting in stabilization of the lactone form of CPT.

All formulations demonstrated high incorporation efficiency (more than about 80%) when liposomes were prepared in acidic conditions (pH 6.0) (Table 1). This could be due to the fact that the stability of the lactone form of the CPT molecule is favored by lower pH conditions than the carboxylate form, which is more hydrophilic at pH 7.0 [29]. Among the formulations examined, DB-L (HSPC/Ch/OA/DB/PEG2000 7:3:1:1:0.4) was most stable after i.v. injection. At present, whether DB interacts with CPT is not clear, but we have reported that the stability of CPT-loaded polymeric micelles in vivo was increased by benzyl esterification of the hydrophobic segment of the block copolymer [11], presumably due to be $\pi-\pi$ interaction of the phenyl group with CPT. DB in liposome membranes, therefore, might interact with CPT by a $\pi-\pi$ interaction and could incorporate CPT into the interior of the bilayers. However, 2DB-L, containing 15 mol% DB, decreased the CPT concentration in plasma compared to DB-L. This suggests that there is an optimal amount of DB for increasing the stability of CPT liposomes, which may be between 8 and 15 mol%. As mentioned above, CPT interacted with DB in liposomal membrane. The incorporation efficiency of DB in liposomes had optimal value. Thus, optimal amount of DB for increasing CPT stability may exist.

The association of some serum protein with opsonic activity has been suppressed in previous studies by pre-coating HSA on the surface of nanoparticles and nanospheres [23,30]. In accord with those observations, HSA-DB-L increased the stability of CPT in the circulation compared to liposomes without HSA on their surface. Carbonyl group of the ring D of CPT may be in liposomes and HSA coating may stabilize them.

CPT solution given as a single i.v. injection at 2.5 mg/kg in tumor-bearing mice often resulted in toxic death, but HSA-DB-L at 15 mg/kg did not cause any significant body weight loss. This finding suggests that HSA-DB-L was up to 6 times less toxic than CPT solution administered by i.v. injection. The pharmacokinetics and tissue distribution data indicated that this reduced toxicity was attributable to lower uptake of CPT in the liver and lung after treatment with HSA-DB-L than after the administration of an equimolar dose of CPT solution. Because of this reduced toxicity, a higher dose of CPT liposomes could be used to treat mice bearing murine colon cancer. HSA-DB-L with low clearance increased the accumulation of CPT in tumor tissue, resulting in increase of the antitumor effect of CPT.

Regarding the therapeutic strategy, it has been shown in nude mice bearing human tumor xenografts that for a fixed total dose, repeated daily administration of CPT conjugated with polymers was far superior to a single injection [31]. Here, our findings suggest that a single injection of HSA-DB-L was effective for suppressing tumor growth at a dose of either 10 or 15 mg/kg ($T/C\%=34.6\%$ and 16.4% at Day 8, respectively). This apparent discrepancy may be due to a difference in the rate of release of free CPT from the liposomes. Although CPT has been shown to be released slowly from CPT conjugated with polymers over several days [31,32], HSA-DB-L released about 20% of its load within 24 h from release test into PBS. These findings suggest that the rapid bioavailability of free CPT from the liposomes may indeed improve antitumor activity subsequent to the passive accumulation of liposomes in the tumor tissue.

DB was not cytotoxic, and therefore the antitumor effect of HSA-DB-L may have been due to CPT. Furthermore, we have synthesized DB derivatives and investigated the interaction between the dodecyloxy group of DB and the lactone ring of CPT to estimate the distribution of CPT in liposomes containing DB. These results were reported as separate manuscript [33].

The results from the biodistribution study revealed that the intravenously injected HSA-DB-L accumulated in the tumor. Drug carriers with a prolonged circulation time can increase the drug accumulation in tumor tissues by the EPR effect, and consequently improve the antitumor activity. Although pegylated liposome, HSA-DB-L seemed to contribute improved CPT solubility in lipids over long circulating, these results suggest that HSA-DB-L with stable property in blood possesses the ability to deliver large amounts of CPT to the tumor site. Here further studies with human tumor xenografts will be required to evaluate the activity of HSA-DB-L.

5. Conclusion

CPT liposomes formulated with DB increased the CPT stability in vitro and in vivo. Furthermore, CPT liposomes coated with HSA prolonged the blood circulation time. This formulation enhanced the accumulation of CPT in tumor tissue, resulting in a significantly higher antitumor effect than CPT solution even with a single injection. This finding will permit the utilization of CPT, which is not now used in clinical practice due to the lack of a suitable drug carrier system.

Acknowledgements

This study was supported in part by the Ministry of Education, Culture, Sports, Science and Technology, Japan, and by the Open Research Center Project. We are grateful to Ms. S. Katayama, Ms. C. Fujita and Ms. M. Katori for technical assistance.

References

[1] M.E. Wall, M.C. Wani, C.E. Cook, K.H. Palmer, A.T. Mcphail, G.A. Sim, Plant antitumor agents: I. The isolation and structure of camptothecin, a novel alkaloidal leukemia and tumor inhibitor from Camptotheca acuminate, J. Am. Chem. Soc. 88 (1966) 3888–3890.

[2] B.C. Giovanella, J.S. Stehlin, M.E. Wall, M.C. Wani, A.W. Nicholas, L.F. Liu, R. Silber, M. Potmesil, DNA topoisomerase I-targeted chemotherapy of human colon cancer in xenografts, Science 246 (1989) 1046–1048.

[3] B.C. Giovanella, H.R. Hinz, A.J. Kozielski, J.S. Stehlin Jr., R. Silber, M. Potmesil, Complete growth inhibition of human cancer xenografts in nude mice by treatment with 20-(*S*)-camptothecin, Cancer Res. 51 (1991) 3052–3055.

[4] R.P. Hertzberg, M.J. Caranfa, S.M. Hecht, On the mechanism of topoisomerase I inhibition by camptothecin: evidence for binding to an enzyme–DNA complex, Biochemistry 28 (1989) 4629–4638.

[5] J. Fassberg, V.J. Stella, A kinetic and mechanistic study of the hydrolysis of camptothecin and some analogues, J. Pharm. Sci. 81 (1992) 676–684.

[6] Z. Mi, T.G. Burke, Differential interactions of camptothecin lactone and carboxylate forms with human blood components, Biochemistry 33 (1994) 10325–10336.

[7] K. Akimoto, A. Kawai, K. Ohya, Kinetic studies of the hydrolysis and lactonization of camptothecin and its derivatives, CPT-11 and SN-38, in aqueous solution, Chem. Pharm. Bull. 42 (1994) 2135–2138.

[8] B.A. Hanson, R.L. Schowen, V.J. Stella, A mechanistic and kinetic study of the E-ring hydrolysis and lactonization of a novel phosphoryloxymethyl prodrug of camptothecin, Pharm. Res. 20 (2003) 1031–1038.

[9] T.G. Burke, A.E. Staubus, A.K. Mishra, Liposomal stabilization of camptothecin's lactone ring, J. Am. Chem. Soc. 114 (1992) 8318–8319.

[10] R. Cortesi, E. Esposito, A. Maietti, E. Menegatti, C. Nastruzzi, Formulation study for the antitumor drug camptothecin: liposomes, micellar solution, and a microemulsion, Int. J. Pharm. 159 (1997) 95–103.

[11] M. Watanabe, K. Kawano, M. Yokoyama, P. Opanasopit, T. Okano, Y. Maitani, Preparation of camptothecin-loaded polymeric micelles and evaluation of their incorporation and circulation stability, Int. J. Pharm. 308 (2006) 183–189.

[12] K. Kawano, M. Watanabe, T. Yamamoto, M. Yokoyama, P. Opanasopit, T. Okano, Y. Maitani, Enhanced antitumor effect of camptothecin loaded in long-circulating polymeric micelles, J. Control. Release 112 (2006) 329–332.

[13] A. Shenderova, T.G. Burke, S.P. Schwendeman, The acidic microclimate in poly(lactide-co-glycolide) microspheres stabilizes camptothecins, Pharm. Res. 16 (1999) 241–248.

[14] W. Tong, L. Wang, M.J. D'Souza, Evaluation of PLGA microspheres as delivery system for antitumor agent-camptothecin, Drug Dev. Ind. Pharm. 29 (2003) 745–756.

[15] G.T. Colbern, D.J. Dykes, C. Engbers, R. Musterer, A. Hiller, E. Pegg, R. Saville, S. Weng, M. Luzzio, P. Uster, M. Amantea, P.K. Working, Encapsulation of the topoisomerase I inhibitor GL147211C in pegylated (STEALTH) liposomes: pharmacokinetics and antitumor activity in HT29 colon tumor xenografts, Clin. Cancer Res. 4 (1998) 3077–3082.

[16] C.L. Messerer, E.C. Ramsay, D. Waterhouse, R. Ng, E.M. Simms, N. Harasym, P. Tardi, L.D. Mayer, M.B. Bally, Liposomal irinotecan: formulation development and therapeutic assessment in murine xenograft models of colorectal cancer, Clin. Cancer Res. 10 (2004) 6638–6649.

[17] A. Tanizawa, A. Fujimori, Y. Fujimori, Y. Pommier, Comparison of topoisomerase I inhibition, DNA damage, and cytotoxicity of camptothecin derivatives presently in clinical trials, J. Natl. Cancer Inst. 86 (1994) 836–842.

[18] M. Yokoyama, P. Opanasopit, T. Okano, K. Kawano, Y. Maitani, Polymer design and incorporation methods for polymeric micelle carrier system containing water-insoluble anti-cancer agent camptothecin, J. Drug Target. 12 (2004) 373–384.

[19] P. Opanasopit, M. Yokoyama, M. Watanabe, K. Kawano, Y. Maitani, T. Okano, Block copolymer design for camptothecin incorporation into polymeric micelles for passive tumor targeting, Pharm. Res. 21 (2004) 2001–2008.

[20] Y. Matsumura, H. Maeda, A new concept for macromolecular therapeutics in cancer chemotherapy: mechanism of tumoritropic accumulation of proteins and the antitumor agent smancs, Cancer Res. 46 (1986) 6387–6392.

[21] H. Maeda, The enhanced permeability and retention (EPR) effect in tumor vasculature, The key role of tumor-selective macromolecular drug targeting, Adv. Enzyme Regul. 41 (2000) 189–207.

[22] H. Maeda, J. Wu, T. Sawa, Y. Matsumura, K. Hori, Tumor vascular permeability and the EPR effect in macromolecular therapeutics: a review, J. Control. Release 65 (2000) 271–284.

[23] K. Ogawara, K. Furumoto, S. Nagayama, K. Minato, K. Higaki, T. Kai, T. Kimura, Pre-coating with serum albumin reduces receptor-mediated hepatic disposition of polystyrene nanosphere: implications for rational design of nanoparticles, J. Control. Release 100 (2004) 451–455.

[24] V.S.K. Balagurusamy, G. Ungar, V. Percec, G. Johansson, Rational design of the first spherical supramolecular dendrimers self-organized in a novel thermotropic cubic liquid-crystalline phase and the determination of their shape by X-ray analysis, Am. Chem. Soc. 119 (1997) 1539–1555.

[25] S.C. Yang, L.F. Lu, Y. Cai, J.B. Zhu, B.W. Liang, C.Z. Yang, Body distribution in mice of intravenously injected camptothecin solid lipid nanoparticles and targeting effect on brain, J. Control. Release 59 (1999) 299–307.

[26] D.L. Warner, T.G. Burke, Simple and versatile high-performance liquid chromatographic method for the simultaneous quantitation of the lactone and carboxylate forms of camptothecin anticancer drugs, J. Chromatogr. B Biomed. Sci. Appl. 691 (1997) 161–171.

[27] H. Onishi, Y. Machida, Y. Machida, Antitumor properties of irinotecan-containing nanoparticles prepared using poly(DL-lactic acid) and poly (ethylene glycol)-block-poly(propylene glycol)-block-poly(ethylene glycol), Biol. Pharm. Bull. 26 (2003) 116–119.

[28] S. Takemoto, K. Yamaoka, M. Nishikawa, Y. Takakura, Histogram analysis of pharmacokinetic parameters by bootstrap resampling from one-point sampling data in animal experiments, Drug Metab Pharmacokinet 21 (2006) 458–464.

[29] R.P. Hertzberg, M.J. Caranfa, K.G. Holden, D.R. Jakas, G. Gallagher, M.R. Mattern, S.M. Mong, J.O. Bartus, R.K. Johnson, W.D. Kingsbury, Modification of the hydroxy lactone ring of camptothecin: inhibition of mammalian topoisomerase I and biological activity, J. Med. Chem. 32 (1989) 715–720.

[30] V.P. Torchilin, V.R. Berdichevsky, A.A. Barsukov, V.N. Smirnov, Coating liposomes with protein decreases their capture by macrophages, FEBS Lett. 111 (1980) 184–188.

[31] Y. Zou, Q.P. Wu, W. Tansey, D. Chow, M.C. Hung, C. Charnsangavej, S. Wallace, C. Li, Effectiveness of water soluble poly(L-glutamic acid)-camptothecin conjugate against resistant human lung cancer xenografted in nude mice, Int. J. Oncol. 18 (2001) 331–336.

[32] M. Zamai, M. VandeVen, M. Farao, E. Gratton, A. Ghiglieri, M.G. Castelli, E. Fontana, R. D'Argy, A. Fiorino, E. Pesenti, A. Suarato, V.R. Caiolfa, Camptothecin poly[*n*-(2-hydroxypropyl) methacrylamide] copolymers in antitopoisomerase-I tumor therapy: intratumor release and antitumor efficacy, Mol. Cancer Ther. 2 (2003) 29–40.

[33] Y. Maitani, S. Katayama, K. Kawano, A. Hayama, K. Toma, Artificial lipids stabilized camptothecin incorporated into liposomes, Biol. Pharm. Bull. (in press).

Artificial Lipids Stabilized Camptothecin Incorporated in Liposomes

Yoshie MAITANI,*[a] Sayaka KATAYAMA,[a] Kumi KAWANO,[a] Akihiro HAYAMA,[a] and Kazunori TOMA[b]

[a] *Institute of Medicinal Chemistry, Hoshi University; Shinagawa-ku, Tokyo 142–8501, Japan: and* [b] *The Noguchi Institute; Itabashi-ku, Tokyo 173–0003, Japan.*

Received October 31, 2007; accepted February 12, 2008; published online February 13, 2008

Camptothecin (CPT) has anticancer activity. While only the lactone form of CPT is biologically active, this form exhibits poor aqueous solubility. Pharmaceutical formulation of CPT incorporated in liposomes is of significant importance to develop the therapeutic utilization of CPT. The aim of this study was to increase incorporation efficiency and stability of CPT in liposomes composed of hydrogenated soybean phosphatidylcholine, cholesterol, and oleic acid (7 : 3 : 1, molar ratio), by incorporating three kinds of artificial lipids (DBs) (DB-liposome); 4-*n*-(M12B), 3,5-bis(B12B) and 3,4,5-tris(dodecyloxy)benzoic acid (T12B). The interaction of CPT with DB in the state of liposomes, was examined. In DB-liposomes presenting mean diameters of 150 nm, incorporation efficiency of CPT up to 55% and final drug to lipid molar ratio up to 0.07 were obtained when the liposomes were prepared at a feeding ratio of 1/30 (w/w) CPT/total lipid. However, in the optimal formulations, incorporated DB mol% was different; T12B and D12B were incorporated about one third and half mol% of M12B, respectively. Moreover, we demonstrated that T12B stabilized CPT in liposomes significantly compared with other DBs as measured by CPT release, and by steady state fluorescence polarization degree of CPT using intrinsic fluorescence of CPT. These findings suggested that in addition of contribution of phenyl group of DB, dodecyloxy group may interact strongly with lactone ring of CPT. The capacity to contain CPT interacted with DBs may be limited in liposomes. T12B may be incorporated in the interior of the bilayers, resulting in increase of incorporation stability of CPT. This finding demonstrates a potential application of the novel liposome formulation of CPT in drug delivery.

Key words camptothecin; liposome; artificial lipid; release test; incorporation efficiency; incorporation stability

Camptothecin (CPT) is a naturally occurring cytotoxic alkaloid isolated from the Chinese plant *Camptotheca accuminate*.[1] CPT and some of its analogs have shown a broad spectrum of antitumor activity against many solid tumors in xenografts including colorectal cancer.[2,3] CPT inhibits the enzyme DNA topoisomerase I, initially by noncovalent binding and subsequently by stabilization of the complex through a nucleophilic attack by the enzyme at the acyl position of the CPT lactone ring.[4]

Of significant importance for pharmaceutical formulation is that, while only the lactone form of CPT is biologically active, this form exhibits poor aqueous solubility. The lactone of CPT is converted to carboxylate in a pH-dependent equilibrium.[5] To overcome the aforementioned solubility problems and hydrolytic processes of CPT, several approaches have been investigated. Numerous attempts have been made to prepare water-soluble CPT analogs. The majority of these analogs were less potent in assays both *in vitro* and *in vivo* than the parent drug. In addition to the synthesis of new derivatives and pro-drug products,[6—10] the development of adequate drug carriers is gaining increasing attention. There are many reports about effective formulation and utilization of CPT in cancer therapy by using drug delivery technologies such as liposomes,[11,12] microemulsions,[12] microspheres,[13,14] and inclusion complexes with cyclodextrins.[15] Previously we have reported that the stability of CPT loaded polymeric micelles *in vivo* was increased by benzyl esterification of hydrophobic segment of block copolymer.[16—18] However, long circulation of CPT loaded polymeric micelles *in vivo* was not achieved yet. Other carriers such as liposomes were examined because release of drugs encapsulated in carriers depended on carriers. The designed amphipathic compounds are called artificial lipid, which has similar properties with phospholipid to form vesicles. Therefore, artificial lipid with a phenyl group, *e.g.*, 3,5-bis(dodecyloxy)benzoic acid, was synthesized and added to the liposome formulation. The PEGylated liposomes incorporating CPT were stable *in vivo*.[19] However, there was not enough information about interaction between CPT and artificial lipid molecules in liposomes.

To develop the therapeutic utilization of CPT, it is necessary to prepare liposomes with high incorporation efficiency and stability of CPT. This study demonstrated that incorporation of 5 mol% of 3,4,5-tris(dodecyloxy)benzoic acid increased incorporation efficiency and stability of CPT in liposomes.

MATERIALS AND METHODS

Materials (*S*)-(+)-Camptothecin (CPT), cholesterol (Ch), high performance liquid chromatography (HPLC) grade methanol and tetrahydrofuran (THF) were purchased from Wako Pure Chemicals (Tokyo, Japan). Hydrogenated soybean phosphatidylcholine (HSPC, >90% phosphatidylcholine), and oleic acid (OA) were purchased from NOF Corporation (Tokyo, Japan). 4-*n*-Dodecyloxy benzoic acid (M12B) was purchased from Tokyo Chemical Industry (Tokyo, Japan). 3,5-Bis(dodecyloxy)benzoic acid (B12B) and 3,4,5-tris(dodecyloxy)benzoic acid (T12B) were synthesized as reported previously[20] (Fig. 1). Other chemicals were of reagent grade.

Preparation of Liposomes Liposomes incorporating CPT were prepared as described elsewhere.[19] Briefly, HSPC, Ch, OA, DB and CPT (molar ratio, HSPC : Ch : OA : DB : CPT = 7 : 3 : 1 : 0—3 : 1; weight ratio, total lipid : CPT = 30 : 1) were dissolved in methanol/chloroform mixture (1/4 (v/v)). The solvent was evaporated in a rotary evaporator at 55 °C under stream of N_2 gas. The lipid film containing the drug was hydrated with 2.5 ml of sodium phosphate-buffered solu-

* To whom correspondence should be addressed. e-mail: yoshie@hoshi.ac.jp

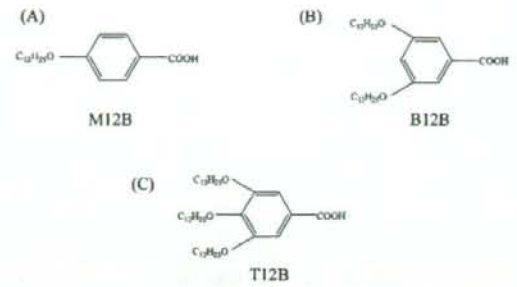

Fig. 1. Chemical Structure of 4-*n*-Dodecyloxy Benzoic Acid (A), 3,5-Bis(dodecyloxy)benzoic Acid (B), and 3,4,5-Tris(dodecyloxy)benzoic Acid (C)

tion (pH 6.04, 2.33% KH_2PO_4 : 1.44% $NaHCO_3$=4 : 1 volume ratio) to protect conversion from the lactone of CPT to carboxylate. The suspension was sonicated for 8 min and was concentrated by centrifugation at 3900 rpm for 10 min to remove the big particles including unentrapped CPT aggregate. Size distribution of liposomes was monitored using a dynamic light scattering particle size analyzer (ELS-800, Otsuka Electronics, Osaka, Japan) at 25 °C by diluting liposome suspensions to an appropriate volume with water.

Determination of CPT and DB Content in Liposomes Drug incorporation efficiency was determined using the ultra-centrifugation method. Liposomes incorporating CPT were centrifuged at 52000 ***g*** for 1 h at 4 °C to separate free CPT. Then, the incorporation efficiency was obtained using two methods: determination of the CPT concentration of the supernatant containing free CPT, and determination of the amount of CPT entrapped in the precipitate, which was disrupted using chloroform. The incorporation efficiencies estimated using both methods were similar. The former method was used in the following experiment. The total drug concentrations in liposomes before centrifugation (liposome A) and in the supernatant after centrifugation (supernatant B) were determined using a F-4010 fluorescence spectrophotometer (Hitachi Electronics, Tokyo, Japan) with the excitation and emission wavelengths of 369 and 437 nm, respectively as described previously.[16]

Incorporation efficiency of DB was determined by HPLC (wavelength at 254 nm). A Shimadzu LC-10AT (Shimadzu Co., Ltd., Japan) apparatus equipped with a Shimadzu RF-10AXL fluorescence detector in which the wavelengths were set at 254 nm. Separation was performed with an YMC-Pack ODS-AA-302 column (150×4.6 mm I.D., YMC Co., Ltd., Kyoto, Japan). For M12B and B12B, the mobile phase was composed of 19 : 1 or 99 : 1 methanol–phosphate-buffered solution (pH 3.02), respectively, and the flow rate was set at 1.0 ml/min. For T12B, 17 : 3 (v/v) methanol–THF. The incorporation efficiency of drug or DB in the liposomes was calculated as follows.

$$\text{incorporation efficiency of drug or DB (\%, w/w)} = \frac{\text{drug (DB)}_{\text{liposome A}} - \text{drug (DB)}_{\text{supernatant B}}}{\text{drug (DB)}_{\text{initial}}} \times 100$$

***In Vitro* Drug Release** *In vitro* release of CPT from the liposomal formulation was analyzed by membrane dialysis against phosphate-buffered saline (PBS, pH 7.4) at 37 °C. Briefly, 1 ml of CPT liposomes was placed in a dialysis tube (Spectra/Por CE (MWCO 12000—14000, Spectrum Laboratories, Inc., Rancho Dominguez, CA, U.S.A.)) and then suspended in a temperature-controlled, jacketed flask containing 100 ml of PBS. After various time intervals, aliquots were withdrawn and assayed for CPT content by fluorophotometry. Drug release profiles (percent release *versus* time) were plotted.

Fluorescence Polarization Measurements To evaluate distribution of CPT in the liposomes, we examined mobility of CPT using intrinsic fluorescence of CPT by fluorescence polarization measurements. We prepared about 10 μM of lipid concentration of M12B-, B12B- and T12B-liposome (HSPC : Ch : OA : M12B : CPT=7 : 3 : 1 : 1 : x, HSPC : Ch : OA : B12B : CPT=7 : 3 : 1 : 1 : x, and HSPC : Ch : OA : T12B : CPT=7 : 3 : 1 : 1 : x, molar ratio) aqueous suspension with CPT concentration varied from 5.7×10^{-1} μg/ml to 0.1 mg/ml (corresponding on x molar ratio). Steady-state fluorescence polarization measurements were performed on F-4500 fluorescence spectrophotometer (HITACHI, Electronics). One-centimeter rectangular quartz fluorometer cell was used, and the excitation and emission wavelengths were set at 369 and 437 nm, respectively. The fluorescence polarization of liposomes in sodium phosphate-buffered solution (pH 6.04) was measured at room temperature (24 °C). $I_{\parallel}$ ($I_{\perp}$) is the intensity of photons with electric vectors parallel (perpendicular) to the beam direction.

$$\text{polarization degree} = \frac{I_{\parallel} - I_{\perp}}{I_{\parallel} + I_{\perp}}$$

Statistical Analysis The statistical significance of the data was evaluated with Student's t test. A p value of 0.05 or less was considered significant.

RESULTS AND DISCUSSION

Preparation and Characterization of CPT Incorporated in Liposomes The incorporation stability of CPT in polymeric micelles *in vitro* and *in vivo* was increased by benzyl esterification of hydrophobic segment of block copolymer, supposed to be π–π interaction of phenyl group with CPT.[16—19] Therefore, the artificial lipids with a phenyl group, DBs were synthesized and added to liposome formulation to obtain stable liposomes incorporating CPT (DB-liposome). Basic formulation, HSPC : Ch : OA : CPT=7 : 3 : 1 : 1 (molar ratio) was decided as HSPC, Ch and OA since liposomes with OA showed about five-fold higher incorporation efficiency of CPT compared with ones without OA.[19] Here we prepared three kinds of liposomes incorporating M12B, B12B and T12B, referred as M12B-, B12B-, and T12B-liposome, respectively. The particle size was not significantly different among all the DB-liposome formulations, and was about 150 nm, when the liposomes were prepared at a feeding ratio of 1/30 CPT/total lipid.

Effect of DB/lipid Ratio on Incorporation to Liposomes CPT and DB contents in liposomes were determined at liposome formulation as HSPC : Ch : OA : DB : CPT=7 : 3 : 1 : 0—3 : 1 (mol), as shown in Figs. 2 and 3. When the ratio of each DB to starting total lipid of M12B-, B12B- and T12B-liposomes was increased to 15.3 mol%, the incorporation efficiency of M12B, B12B and T12B was increased to 84, 61

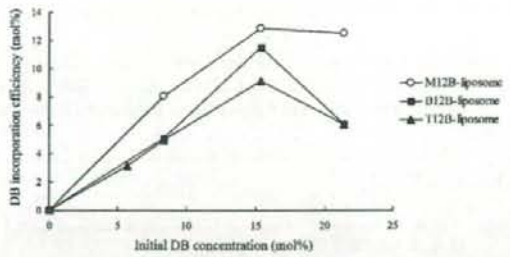

Fig. 2. Effect of Initial DB Concentration on Final DB Incorporation Levels in DB-Liposomes Composed of HSPC : Ch : OA : DB : CPT=7 : 3 : 1 : 0—3 : 1 (Molar Ratio)

Data are average of 2 independent experiments.

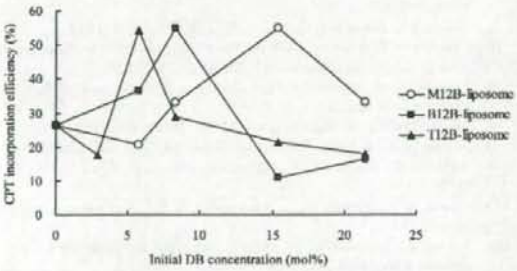

Fig. 3. Effect of Initial DB Concentration on Final CPT Incorporation Efficiency in DB-Liposomes Composed of HSPC : Ch : OA : DB : CPT= 7 : 3 : 1 : 0—3 : 1 (Molar Ratio)

Data are average of 2 independent experiments.

and 54%, respectively (Fig. 2). Also, incorporation efficiency of CPT up to 55% in all liposomes was obtained (Fig. 3). However, in the optimal formulation, DB (mol%) was different. Without DB, 26.3% of CPT was incorporated in liposomes (Control-L). The maximum CPT incorporation efficiency was obtained at the formulations of DB-liposomes: HSPC : Ch : OA : M12B : CPT=7 : 3 : 1 : 2 : 1 (molar ratio, M12B-L), HSPC : Ch : OA : B12B : CPT=7 : 3 : 1 : 1 : 1 (B12B-L), and HSPC : Ch : OA : T12B : CPT=7 : 3 : 1 : 0.67 : 1 (T12B-L), as reflected about 2-fold increase (55% for M12B-L and B12B-L, and 54% for T12B-L, final drug to lipid molar ration up to 0.07) compared with Control-L. Among DB-liposomes, T12B seemed most effective to incorporate CPT in liposomes since it worked at the smallest addition amount. The excess amount of T12B decreased incorporation of CPT in liposomes, suggesting that the capacity to contain the complex of T12B with CPT might be limited in liposomes. When increase of initial CPT amount in T12B-liposomes, the incorporation efficiency of CPT was decreased (data not shown). The incorporation of DBs in liposomes seemed to decide incorporation of CPT in liposomes. Because CPT could not complex with B12B (data not shown), DBs may distribute in liposomes, and then CPT may interact with DBs and could be incorporated into the interior of the bilayers. CPT molecules may be accumulated in hydrophobic region of membranes. The presence of DB contributed increased 30% of incorporation efficiency. These findings suggested that increased CPT incorporation efficiency by DBs might be due to interaction between phenyl and dodecyloxy

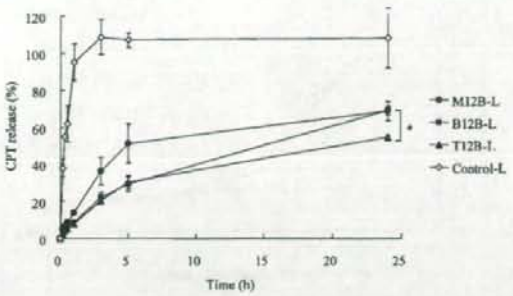

Fig. 4. Percent CPT Released as a Function of Time at 37 °C

CPT release from the liposomes of M12B-L (○), B12B-L (■), T12B-L (▲) and Control-L (◇) at the initial CPT entrapped in liposomes concentration of 200 μg/ml. CPT was monitored by membrane dialysis as described in Materials and Method using PBS as sink solution at pH=7.4. Data are expressed in the mean±standard deviation of 3 independent experiments. * $p<0.05$.

group of DBs and lactone ring of CPT over increase of acidity by carboxyl group of DBs.

***In Vitro* Drug Release** The incorporation stability of CPT in M12B-L, B12B-L and T12B-L was examined from drug release test by incubation in PBS at 37 °C, as shown in Fig. 4. The CPT released from Control-L was 100% for 3 h while that from M12B-L, B12B-L and T12B-L were 36.3, 22.3 and 20.5%, respectively. The CPT released from M12B-L was significantly higher than that from B12B-L and T12B-L for 5 h. CPT incorporated in M12B-L may be distributed at the surface of liposomes more than that in B12B-L and T12B-L, therefore CPT was released highly. During 24-h-period, M12B-L, B12B-L and T12B-L released 68.8, 69.0 and 54.5%, respectively. Release of CPT among DB-liposomes was higher T12B<B12B<M12B, and T12B-L showed significantly lower release than B12B and M12B at 24 h ($p<0.05$). This result indicated that DBs increased incorporation stability of CPT, and incorporation stability of CPT was increased with increase of the numbers of dodecyloxy-group of DBs. Dodecyloxy-group of DBs might induce drug's lactone ring to penetrate into lipid bilayers.

Fluorescence Measurements Anisotropy measurements were worthwhile as a strong indication of incorporation stability. Polarization degree of intrinsic fluorescence of CPT incorporated in the liposomes was evaluated. Figure 5 revealed that the polarization degree was CPT concentration-dependant. The polarization degree values were directly related to the kind of environment where the CPT was distributed. Free rotations in DMSO solution were related to the smallest values of polarization degree, compared to the state in liposomes, indicating that CPT molecule can move freely. M12B-, B12B- and T12B-liposomes at 0.11—0.13 μM of CPT concentration, exhibited higher polarization degree (0.47, 0.45, 0.53, respectively) compared with Control-liposomes. These results reflected that CPT molecules were inserted deeply into the lipid bilayer of liposomes. A pronounced decrease in polarization was observed below about 1 μM CPT in liposomes, revealed disordering of the lipid bilayer in the presence of CPT. Among DB-liposomes, T12B-liposome seemed to have high incorporation stability, resulting from protection of disordering property of CPT in liposomes. This result corresponded with that of release test;

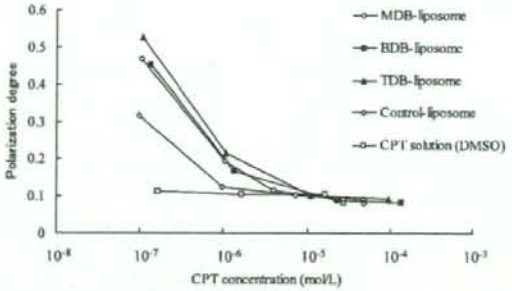

Fig. 5. Polarization Degree *versus* CPT Concentration Incorporated in M12B-Liposome (○), B12B-Liposome (■), T12B-Liposome (▲) Control-Liposome (◇) and CPT DMSO Solution at Room Temperature (24 °C)

M12B-, B12B- and T12B-liposome (HSPC : Ch : OA : M12B : CPT = 7 : 3 : 1 : 1 : *x*, HSPC : Ch : OA : B12B : CPT = 7 : 3 : 1 : 1 : *x* and HSPC : Ch : OA : T12B : CPT = 7 : 3 : 1 : 1 : *x*, molar ratio, respectively) aqueous suspension with CPT concentration varied from 5.7×10^{-1} μg/ml to 0.1 mg/ml.

CPT in T12B-L showed the lowest release among DB-liposomes. These findings suggested that CPT in T12B-L would be incorporated into the interior of the bilayers by interaction of dodecyloxy-group of T12B with drug's lactone ring, and release slowly, while CPT in Control-L would be in contact with the water/lipid interface, be changed into the ionized form, and be released quickly.

Liposomal CPT delivery systems may be promising to cancer therapy. We have reported presently to apply this PE-Gylated formulation *in vivo* to evaluate anticancer effect.[19]

CONCLUSIONS

By incorporating various amounts of artificial lipid, DB, incorporation efficiency of CPT in liposomes increased. Additionally, we demonstrated, 4,5-tris(dodecyloxy)benzoic acid (T12B) stabilized significantly CPT in liposomes at about one third of M12B amount compared with other DBs as measured by CPT release. These findings suggested that incorporation stability of CPT in liposomes was increased, likely due to the interaction between lactone ring of CPT and dodecyloxy group more than phenyl group of DB, resulting in CPT incorporated into the interior of the bilayers.

Acknowlegements This study was supported in part by the Ministry of Education, Culture, Sports, Science and Technology of Japan, and by the Open Research Center Project.

REFERENCES

1) Wall M. E., Wani M. C., Cook C. E., Palmer K. H., Mcphail A. T., Sim G. A., *J. Am. Chem. Soc.*, **88**, 3888—3890 (1966).
2) Giovanella B. C., Stehlin J. S., Wall M. E., Wani M. C., Nicholas A. W., Liu L. F., Silber R., Potmesil M., *Science*, **246**, 1046—1048 (1989).
3) Giovanella B. C., Hinz H. R., Kozielski A. J., Stehlin J. S., Silber R., Potmesil M., *Cancer Res.*, **51**, 3052—3055 (1991).
4) Hertzberg R. P., Caranfa M. J., Hecht S. M., *Biochemistry*, **28**, 4629—4638 (1989).
5) Fassberg J., Stella V. J., *J. Pharm. Sci.*, **81**, 676—684 (1992).
6) Conover C. D., Greenwald R. B., Pendri A., Gilbert C. W., Shum K. L., *Cancer Chemother. Pharmacol.*, **42**, 407—414 (1998).
7) Fleming A. B., Haverstick K., Saltzman W. M., *Bioconjug. Chem.*, **15**, 1364—1375 (2004).
8) Mi Z., Burke T. G., *Biochemistry*, **33**, 10325—10326 (1994).
9) Warnecke A., Kratz F., *Bioconjug. Chem.*, **14**, 377—387 (2003).
10) Akimoto K., Kawai A., Ohya K., *Chem. Pharm. Bull.*, **42**, 2135—2138 (1994).
11) Daoud S. S., Fetouh M. I., Giovanella B. C., *Anticancer Drugs*, **6**, 83—93 (1995).
12) Cortesi R., Esposito E., Maietti A., Menegatti E., Nastruzzi C., *Int. J. Pharm.*, **159**, 95—103 (1997).
13) Shenderova A., Burke T. G., Schwendeman S. P., *Pharm. Res.*, **16**, 241—248 (1997).
14) Tong W., Wang L., D'souza M. J., *Drug Dev. Ind. Pharm.*, **29**, 745—756 (2003).
15) Kang J., Kumar V., Yang D., Chowdhury P. R., Hohl R. J., *Eur. J. Pharm. Sci.*, **15**, 163—170 (2002).
16) Kawano K., Watanabe M., Yamamoto T., Yokoyama M., Opanasopit P., Okano T., Maitani Y., *J. Controlled Release*, **112**, 329—332 (2006).
17) Opanasopit P., Yokoyama M., Watanabe M., Kawano K., Maitani Y., Okano T., *Pharm. Res.*, **21**, 2001—2008 (2004).
18) Watanabe M., Kawano K., Yokoyama M., Opanasopit P., Okano T., Maitani Y., *Int. J. Pharm.*, **308**, 183—189 (2006).
19) Watanabe M., Kawano K., Toma K., Hattori Y., Maitani Y., *J. Controlled Release*, in press.
20) Hara M., Takanashi Y., Tuzuki N., Kawakami H., Toma K., Higuchi A., *Cytotechnology*, **42**, 13—20 (2003).

Design of Folate-Linked Liposomal Doxorubicin to its Antitumor Effect in Mice

Atsushi Yamada,[1] Yukimi Taniguchi,[1] Kumi Kawano,[1] Takashi Honda,[2] Yoshiyuki Hattori,[1] and Yoshie Maitani[1]

Abstract

Purpose: Tumor cell targeting is a promising strategy for enhancing the therapeutic potential of chemotherapy agents. Polyethylene glycol (PEG)-coated (sterically stabilized) liposomes show enhanced accumulation on the surface of tumors, but steric hindrance by PEGylation reduces the association of the liposome-bound ligand with its receptor. To increase folate receptor (FR) targeting, we optimized the concentration and PEG spacer length of folate-PEG-lipid in liposomes.

Experimental Design: Three types of folate-linked liposomal doxorubicin were designed and prepared by optimizing the concentration and PEG spacer length of folate-PEG-lipid in PEGylated or non-PEGylated liposomes and by masking folate-linked liposomes where the folate ligand is "masked" by adjacent PEG spacers. The liposome targeting efficacy was evaluated *in vitro* and *in vivo*.

Results: In human oral carcinoma KB cells, which overexpress FR, modification with sufficiently long PEG spacer and a high concentration of folate ligand to non-PEGylated liposomes increased the FR-mediated association and cytotoxicity more than with PEGylated and masked folate-linked liposomes. On the contrary, in mice bearing murine lung carcinoma M109, modification with the folate ligand in PEGylated and masked folate-linked liposomes showed significantly higher antitumor effect than with non-PEGylated liposomes irrespective of the length of time in the circulation after intravenous injection.

Conclusions: The results of this study will be beneficial for the design and preparation of ligand-targeting carriers for cancer treatment.

A variety of targeting ligands have been examined in tumor-targeted drug carriers. Folate receptor (FR)-α is a glycosyl phosphatidylinositol-anchored membrane protein that is selectively overexpressed in >90% of ovarian carcinomas (1–3), and to various extents in other epithelial cancers, but is only minimally distributed in normal tissues (2, 4–6). FR can serve as an excellent tumor marker as well as a functional tumor-specific receptor. Folic acid, a high-affinity ligand for FR, retains its receptor-binding and endocytosis properties even if it is covalently linked to a wide variety of molecules. Therefore, liposomes conjugated to the folate ligand via a polyethylene glycol (PEG) spacer have been used to deliver chemotherapeutic agents, oligonucleotides, and markers to FR-bearing tumor cells (7–16). The targeting efficiency of folate-linked vesicles was affected by the amount of folate-PEG-lipid. It was reported that a higher molar fraction of folate-PEG-lipid in folate-linked liposomes reduced liposome uptake into cells (17). Folate molecules can form dimers, trimers, and even self-assembling tubular quartets at higher concentrations (18). Because FR can only bind one molecule of folic acid (19), such self-assembled multimers of folic acid are incapable of binding to FR.

PEGylated liposomes, called sterically stabilized liposomes, evade uptake by the reticuloendothelial system and show enhanced accumulation in tumors as a result of an enhanced permeability and retention effect. Liposomes were modified with folate to further increase targeting to FR and drug uptake by tumors. However, when targeting moieties are employed, circulation times are often decreased *in vivo* due to recognition by the reticuloendothelial system (9). As a result, the advantage of increased drug retention on the tumor surface by PEGylation is obscured by accelerated clearance of folate-linked formulations. Furthermore, steric hindrance by PEGylation reduces the association of the liposome-bound ligand with its receptor (8). Therefore, the density and PEG spacer length of the targeting ligand and PEGylation of liposomes are known to be critical characteristics for ligand-receptor interaction. However, there have been few studies concerned with the optimization of these factors.

In our previous studies, we have reported on the optimal folate concentration and PEG spacer length with nanoemulsions and polymer micelles (20, 21). However, in these cases,

Authors' Affiliations: [1]Institute of Medicinal Chemistry, Hoshi University, Tokyo, Japan and [2]Fukushima Medical University School of Nursing, Fukushima-City, Japan

Received 1/21/08; revised 5/16/08; accepted 6/6/08.

Grant support: Ministry of Education, Culture, Sports, Science and Technology, Japan, Ministry of Health, Labor and Welfare, Japan, and Open Research Center Project.

The costs of publication of this article were defrayed in part by the payment of page charges. This article must therefore be hereby marked *advertisement* in accordance with 18 U.S.C. Section 1734 solely to indicate this fact.

Note: Supplementary data for this article are available at Clinical Cancer Research Online (http://clincancerres.aacrjournals.org/).

Requests for reprints: Yoshie Maitani, Institute of Medicinal Chemistry, Hoshi University, Shinagawa, Ebara 2-4-41, Tokyo, 142-8501 Japan. Phone: 81-3-5498-5048; Fax: 81-3-5498-5048. E-mail: yoshie@hoshi.ac.jp.

doi:10.1158/1078-0432.CCR-08-0159

Translational Relevance

PEGylated liposomes show enhanced accumulation on the surface of tumors by long circulation. FR is selectively overexpressed to various extents in epithelial cancers. Folic acid is a high-affinity ligand for FR. The targeting efficiency of folate-linked vesicles was affected by the amount of both folate-PEG-lipid and PEG-lipid. To increase FR targeting, we optimized the concentration and PEG spacer length of folate-PEG-lipid in liposomes. In mice bearing murine lung carcinoma M109, modification with the folate ligand in PEGylated and masked folate-linked liposomes where the folate ligand is "masked" by adjacent PEG spacers showed significantly higher antitumor effect than with non-PEGylated liposomes after intravenous injection. This finding suggested that tumor targeting was achieved by less PEGylated carriers with ligand. Three anthracycline liposomal preparations including PEGylated liposomal doxorubicin (Doxil) are currently on the market, and many other liposomal formulations of antineoplastic drugs are in preclinical or clinical trials. Therefore, this strategy will be applied to such drug formulations for future practice of cancer medicine. The results of this study will be beneficial for the design and preparation of ligand-targeting carriers to deliver chemotherapeutic agents and gene for cancer treatment and contrast agents for the detection of solid tumors.

PEG-lipid and PEG polymer are the main components that form the nanoemulsions and polymer micelles, respectively, so we could not evaluate effect of folate-PEG-lipid alone on targeting to tumors. Because liposomes can be prepared without PEG-lipid, we can estimate the optimal density and PEG spacer length of folate-PEG-lipid for FR targeting to produce a balance between longer circulation time and FR targeting.

Here, we designed and prepared various folate-linked liposomes to increase the level of FR-targeting. In this study, we evaluated folate-mediated association of liposomal doxorubicin with human oral carcinoma KB cells and murine lung carcinoma M109 cells, which both overexpresses FR, in terms of the effect of PEG spacer length and the ratio of modification of the folate ligand of liposomes with or without PEG-coating and of the degree of masking of folate ligands on liposomes by adjacent PEG. Furthermore, the antitumor effect of these liposome preparations was investigated *in vitro* and *in vivo*.

Materials and Methods

Materials. Hydrogenated soybean phosphatidylcholine (HSPC) was obtained and amino-PEG-distearylphosphatidylethanolamine (amino-PEG-DSPE; PEG mean molecular weights, 2,000, 3,400, and 5,000) and methoxy-PEG-distearylphosphatidylethanolamine (mPEG-DSPE; PEG mean molecular weights, 2,000 and 5,000) were kind gifts from the NOF. Cholesterol, doxorubicin hydrochloride, and high-performance liquid chromatography-grade acetonitrile were purchased from Wako Pure Chemical Industries. Folate-PEG-DSPEs (F-PEG_{2000}-DSPE, F-PEG_{3400}-DSPE, and F-PEG_{5000}-DSPE), which are conjugates of folic acid and amino-PEG-DSPE, were synthesized as reported previously (8, 20). Folate-deficient RPMI 1640 and fetal bovine serum were obtained from Invitrogen. Other reagents used in this study were of reagent grade.

Preparation of folate-linked liposomal doxorubicin. Liposomes were prepared from hydrogenated soybean phosphatidylcholine/cholesterol = 55/45 (mol/mol) by a dry-film method. Briefly, all lipids were dissolved in chloroform, which was removed by evaporation. The thin film was hydrated with citrate buffer (300 mmol/L, adjusted to pH 4.0 with NaOH) at 60°C by vortex mixing and sonication. Targeted formulations were prepared by mixing nontargeted liposomes with micelles of mPEG-DSPE and/or F-PEG-DSPE to allow incorporation of targeting ligands at 60°C for 1 h by the postinsertion technique (22). The number of targeting ligands was controlled by altering the concentration of micelles added to the liposomes before loading with doxorubicin.

Schematic diagrams (Fig. 1) show three kinds of folate-PEG-liposomes: overhanging folate outside non-PEGylated liposomes (NL), PEGylated liposomes with a $mPEG_{2000}$ layer (SL), and masked folate inside a $mPEG_{5000}$ layer of liposomes (ML). NLs with folate ligands were prepared by incubation of NL with an aqueous dispersion of F-PEG-DSPE (from 0.01 to 0.5 mol% total lipids; Fig. 1A). SLs modified with folate were prepared by incubation of NLs with a total of 2.5 mol% PEG-lipids of $mPEG_{2000}$-DSPE and varying percentages of F-PEG_{5000}-DSPE (F5; Fig. 1B). MLs were prepared by incubation of NLs with an aqueous dispersion of 0.25 mol% F-PEG_{2000}-DSPE and 0.75 mol% $mPEG_{5000}$-DSPE (Fig. 1C). NLs linked with F-PEG_{2000}-DSPE, F-PEG_{3400}-DSPE, or F-PEG_{5000}-DSPE are henceforth abbreviated as F2-NL, F3-NL, and F5-NL, respectively, and SL linked with F-PEG_{5000}-DSPE is abbreviated as F5-SL. The number before the abbreviated term of F5-NL in some descriptions indicates the mol% F-PEG-DSPE of total lipids. For instance, 0.25F5-NL indicates liposomes with 0.25 mol% F-PEG_{5000}-DSPE of total lipids, and 0.25F5-SL indicates liposomes with total 2.5 mol% PEG-lipids composed of 2.25 mol% $mPEG_{2000}$-DSPE for steric stabilization and 0.25 mol% F-PEG_{5000}-DSPE. The resulting mean diameter and ζ potential of liposomes were determined by dynamic light scattering and electrophoresis methods, respectively (ELS-800; Otsuka Electronics) at 25°C after diluting the liposome suspension with water.

Next, these liposomes were actively loaded with doxorubicin by a pH gradient method (23). After the external pH was adjusted to pH 7.4, liposomes were incubated with doxorubicin [drug/lipid = 1:5 (w/w)] at 60°C for 25 min. Doxorubicin loading efficiency was determined by separating unencapsulated from encapsulated drug on a Sephadex G-50 column. Doxorubicin concentration was determined by measuring absorbance at 480 nm (UV-1700 Phamaspec; Shimadzu). The final liposomal doxorubicin was suspended in 150 mmol/L NaCl. The final total lipid concentration of folate-linked liposomes was 18.6 mg/mL.

In vitro drug release of liposomes. *In vitro* release of doxorubicin from the liposomal formulation was analyzed by membrane dialysis against PBS (pH 7.4) at 37°C under sink condition. Briefly, 1 mL liposomal doxorubicin (0.2 mg/mL doxorubicin) was placed in a dialysis tube (seamless cellulose tube membranes; Viskase Sales) with a molecular weight cutoff of 12,000 to 14,000 and then suspended in a temperature-controlled, jacketed flask containing 100 mL PBS. After various time intervals, aliquots of the medium were withdrawn. The doxorubicin concentration was analyzed using a fluorophotometer (Wallac 1420 ARVOsx multilabel counter; Perkin-Elmer Life Science) with excitation and emission wavelengths of 485 and 535 nm, respectively.

Cell culture. KB cells were obtained from the Cell Resource Center for Biomedical Research, Tohoku University. The human lung adenocarcinoma A549 cell line [FR(-)] was kindly provided by OncoTherapy Science. The cells were cultured in folate-deficient RPMI 1640 with 10% heat-inactivated fetal bovine serum and 50 μg/mL kanamycin sulfate in a humidified atmosphere containing 5% CO_2 at 37°C. The cells were prepared by plating 3×10^5 per well in a 12-well culture plate for flow cytometry analysis or 1×10^4 per well in a 96-well culture plate for cytotoxicity analysis for 1 day before the assay.

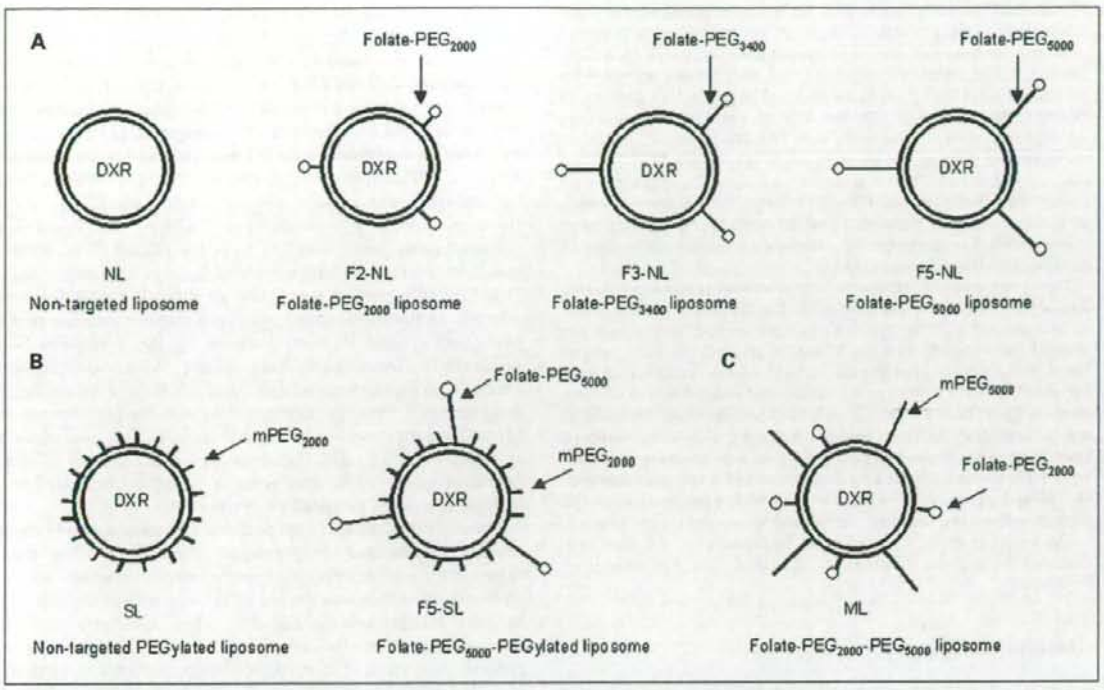

Fig. 1. Schematic diagrams of folate-linked liposomal doxorubicin (*DXR*).

Murine lung carcinoma M109 cells (high FR-expressing cell line) were obtained from Division Chemotherapy (Translational Research Center), Chiba Cancer Center. M109 cells were used to evaluate the accumulation of folate-linked liposomes in tumor tissue and therapeutic effect. The cells were subcultured by employing the biogenic system of BALB/c mice.

Cellular uptake of liposomal doxorubicin assessed by flow cytometry. KB and A549 cells were incubated with liposomal doxorubicin containing 20 μg/mL doxorubicin diluted in 1 mL medium for 1 h at 37°C. In free folate competition studies, 1 mmol/L folic acid was added to the medium. After incubation, the cells were washed with cold PBS (pH 7.4) three times, detached with 0.02% EDTA-PBS for KB cells and with 0.05% trypsin for A549 cells, and then suspended in PBS containing 0.1% bovine serum albumin and 1 mmol/L EDTA. The suspended cells were directly introduced into a FACSCalibur flow cytometer (Becton Dickinson) equipped with a 488 nm argon ion laser. Data for 10,000 fluorescent events were obtained by recording forward scatter, side scatter, and 585/42 nm fluorescence. The autofluorescence of cells incubated with medium without drugs for 1 h was taken as a control.

Confocal laser scanning microscopy. After incubation with liposomes containing 20 μg/mL doxorubicin for 1 h, the medium was removed, and the cells were washed three times with PBS and fixed with 10% formaldehyde PBS at 37°C for 20 min. Then, the cells were coated with Aqua Poly/Mount (Polyscience) to prevent fading and covered with coverslips. The fixed cells were observed with a Radiance 2100 confocal laser scanning microscope (Bio-Rad).

In vitro *cytotoxicity study.* KB cells were incubated with liposomal doxorubicin containing 0.02 to 100 μg/mL doxorubicin diluted in 100 μL medium for 2 h at 37°C. After incubation, the cells were washed with cold PBS (pH 7.4) and cultured in fresh medium for 48 h. Then, 10 μL WST-8 (Dojindo Laboratories) stock solution (5 mmol/L) was added to each well, and the plate was incubated for 1 h at 37°C. Cell viability was assessed by measuring the absorbance at 450 nm.

Pharmacokinetic analysis. Male ddY mice (body weight, ~28 g) were obtained from Tokyo Laboratory Animal Science. Liposomes were injected as a single intravenous bolus via the lateral tail vein at a dose of 5 mg/kg doxorubicin. At 3, 6, and 24 h after the injection, blood was collected and centrifuged to obtain serum. Serum doxorubicin levels were determined by a high-performance liquid chromatography method (24). The high-performance liquid chromatography system was composed of a LC-10AS pump (Shimadzu), a SIL-10A autoinjector (Shimadzu), a RF-10A_{XL} fluorescence detector (excision, 482 nm; emission, 550 nm; Shimadzu), and a YMC-Pack ODS-A, 150 × 4.6 mm i.d. column (YMC). The mobile phase was 0.1 mol/L ammonium formate (pH 4.0)/acetonitrile [7:3 (v/v)] with a flow rate of 1.0 mL/min. The concentration of doxorubicin in each sample was determined using a calibration curve, with daunomycin as the internal standard. Pharmacokinetic variables were calculated using a bootstrap method, including area under the concentration curve (from 3 to 24 h; AUC) and clearance (25).

Microscopic imaging of tumor section. M109 cells were inoculated subcutaneously into female CDF_1 mice (5 weeks old; Sankyo Lab Service). When the tumor volume reached ~100 mm^3, each preparation of liposomes, SL, 0.25F5-SL, ML, and free doxorubicin, was injected intravenously at 5 mg/kg doxorubicin body weight. Twenty-four hours after liposome injection, the mice were sacrificed, and tumor tissues were collected and immediately frozen in dry ice. The tumors were embedded in OCT compound (Tissue-Tek; Sakura Finetechnical) and processed by frozen sectioning at 10 μm. Each frozen section was mounted on a MAS-coated slide glass (SUPER-FROST; Matsunami). The specimens were fixed in 4% paraformaldehyde for 15 min at room temperature and washed three times with

PBS-0.02% Tween 20. Protein blocking was done for 30 min at room temperature using PBS-0.02% Tween 20 containing 0.3% skimmed milk, and the specimens were then washed three times with PBS-0.02% Tween 20. The specimens were incubated with biotin-conjugated rat anti-mouse CD31 (PECAM-1) monoclonal antibody (BD Biosciences Pharmingen), diluted 1:200, for 1 h at room temperature and subsequently washed three times with PBS-0.02% Tween 20. Immunofluorescent staining was done by using streptavidin-FITC (Invitrogen), diluted to 1:200, for 1 h at room temperature. The specimens were washed for a final time with PBS-0.02% Tween 20, and coverslips were mounted on the glass slides with prolong Antifade (Aqua Poly/Mount; Polysciences). The specimens were examined microscopically using an ECLIPSE TS100 microscope (Nikon).

Therapeutic studies. M109 cells were inoculated subcutaneously into female CDF_1 mice (5 weeks old; Sankyo Lab Service). When the tumor volume reached ~100 to 200 mm^3, each preparation of liposomes was injected intravenously at 8 or 10 mg/kg doxorubicin body weight. Liposomal doxorubicin or free doxorubicin solution was injected via a lateral tail vein. The control group was injected with saline (0.1 mL/10 g body weight). Tumor volumes and body weight were measured at regular intervals. The tumor size was measured with vernier calipers. Tumor volume was calculated using the following equation: volume = $\pi / 6 \times LW^2$, where L is the long diameter and W is the short diameter. The animal experiments were done with ethical approval from the Institutional Animal Care and Use Committee at Hoshi University.

Statistical analysis. The statistical significance of the data was evaluated by analysis of Student's t test. $P \leq 0.05$ was considered significant.

Results and Discussion

We supposed that active targeting by folate modification could be achieved based on success in passive targeting of drug carriers by PEGylation. To optimize folate presentation, the design of folate-linked liposomes used in this study is presented in Fig. 1. We prepared three kinds of folate-linked liposomes: overhanging folate-linked NL and SL and masking folate-linked ML. For overhanging folate-linked liposomes, we used various concentrations and PEG spacer lengths of F-PEG-DSPE to attain high-affinity binding. Accordingly, liposomal formulations were characterized for their *in vitro* efficacy of drug delivery and for their *in vivo* pharmacokinetics and tumor therapeutic efficacy. Optimal formulation of folate-linked liposomes was achieved by optimizing the folate ligand density and PEG spacer length on the surface of the liposomes.

Preparation of folate-linked liposomal doxorubicin. For efficient drug delivery to the target site, drugs should be stably entrapped in liposomes. In this study, the sequence of processes of folate modification on the liposome and doxorubicin loading was examined to efficiently encapsulate doxorubicin in liposomes. We used three kinds of procedures: (A), (*a*) folate modification on liposomes, (*b*) pH gradient by changing the outside pH, and (*c*) doxorubicin loading; (B), (*a*) pH gradient by changing the outside pH, (*b*) doxorubicin loading, and (*c*) folate modification on liposomes; (C), (*a*) pH gradient by changing the outside pH, (*b*) folate modification on liposomes, and (*c*) doxorubicin loading. The liposomes prepared using procedures (A) to (C) exhibited 95%, 15.6%, and 7.3% entrapment efficiencies of doxorubicin, respectively. This finding suggested that folate modification on liposomes affected the liposomal membrane, resulting in a decrease in the pH gradient and then a decrease in the entrapment of doxorubicin. Doxorubicin loading after folate modification gave a high entrapment efficiency of >95% at a drug-to-total lipid ratio of 1:5 (w/w), corresponding with the previous report (26). Hereafter, we used procedure (A) for doxorubicin entrapment. In all cases, the average particle diameter of each liposome was ~100 nm with a narrow, monodisperse distribution and ζ potential of -9 to -14 mV.

Effect of F-PEG-DSPE in folate-linked liposomal doxorubicin on cellular uptake and drug release. First of all, the time dependency of the amount of folate-linked liposomes associated with the cells was evaluated by fluorescence of doxorubicin in cells (Supplementary Fig. S1). Flow cytometry analysis showed a shift in the curve, indicating a clear increase in cellular association of folate-linked liposomes after incubation. Until the second hour of incubation, the cellular association of folate in F5-NL increased with the increasing amount of folate more than NL. The associated amount of doxorubicin in F5-NL reached a plateau after 2 to 3 h. Because folate-linked liposomes rapidly associate with FR overexpressed KB cells, it was clarified that typical saturation was achieved within the second hour of incubation (27). Thereafter, incubation for 1 h was used in the following experiments.

Next, we examined the optimal concentration and PEG spacer length of F-PEG-DSPE in liposomes for cellular uptake. For the influence of the PEG spacer length to uptake, a larger PEG spacer, F-PEG_{5000}-DSPE, showed higher association after a 1 h incubation (Fig. 2A). With regard to the density of F-PEG-DSPE, the highest level of folate modification (0.5 mol%) showed the highest uptake regardless of PEG spacer length except for F5-NL. F5-NL with 0.25 mol%

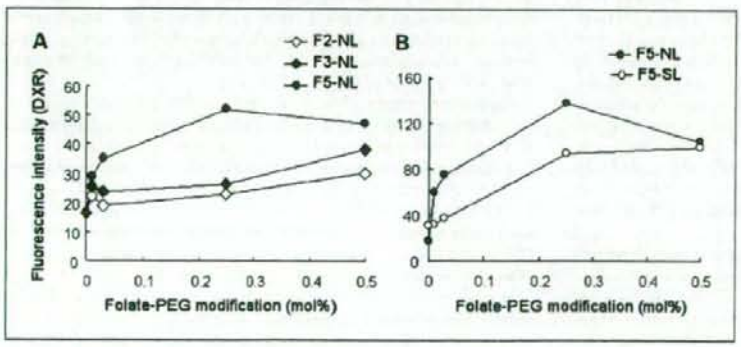

Fig. 2. Dependency of cellular association of non-PEGylated (*A*) and PEGylated (*B*) liposomal doxorubicin on folate-PEG concentration. Cell-associated doxorubicin was determined by flow cytometry analysis after KB cells were incubated with 20 μg/mL doxorubicin for 1 h at 37°C. Each analysis was generated by counting 10^4 cells.

Table 1. IC_{50} of folate-linked liposomal doxorubicin with KB cells

Formulation	IC_{50} (μg/mL)
Free doxorubicin	0.65
NL	2.39
0.25F5-NL	1.15
SL	3.37
0.03F5-SL	2.70
0.25F5-SL	1.27
ML	1.62

NOTE: Mean (n = 5).

F-PEG-DSPE had the highest association rate, showing ~3-fold greater association than nontargeted liposomes (NL). Furthermore, we compared the uptake of NL and SL modified with F-PEG_{5000}-DSPE, with the NL form showing the highest uptake (Fig. 2B). The association of 0.25F5-SL was reduced in comparison with 0.25F5-NL. Therefore, we selected 0.25F5-SL and 0.25F5-NL and compared with ML.

To compare cellular uptake of three types of liposomes, stability was evaluated by drug release. 0.25F5-SL, 0.25F5-NL, and ML were not leaky because <2% drug release was observed over a 8 h incubation period at 37°C (Supplementary Fig. S2). This result indicates that the quantity of folate modification did not affect the stability of liposomal doxorubicin.

Cellular uptake of 0.25F5-SL, 0.25F5-NL, and ML was examined in FR(+) KB and FR(-) A549 cells by flow cytometry. Cellular association of doxorubicin to KB cells was higher ML < 0.25F5-SL < 0.25F5-NL irrespective of the same 0.25 mol% folate modification (Supplementary Fig. S3). Additionally, these increased associations of 0.25F5-SL and 0.25F5-NL to KB cells could be completely blocked by adding 1 mmol/L free folic acid to the medium, but those of ML was not changed. Lower association of 0.25F5-SL and 0.25F5-NL to A549 cells was observed compared with that to KB cells, but similar association of ML was observed to both cells. PEG layer may disturb interaction of folate with FR; therefore, ML may be effectively masked by folate ligand because of less uptake nevertheless low concentration of PEG coating than 0.25F5-SL.

To investigate difference of cellular uptake among 0.25F5-SL, 0.25F5-NL, and ML, the intracellular localization of the liposomes was observed by confocal laser scanning microscopy. Fluorescence images of KB and A549 cells after incubation with liposomes for 1 h are shown in Supplementary Fig. S4. Doxorubicin fluorescence was detected as red color within cells. Higher cellular uptake of 0.25F5-SL and 0.25F5-NL to KB cells was observed than that to A549 cells, whereas ML was not taken up to both cells. This indicated that, similar to result from cellular uptake by flow cytometry, ML was masked efficiently to KB cells.

Effect of F-PEG-DSPE in folate-linked liposomal doxorubicin on cytotoxicity. To confirm the optimal density and PEG spacer length of F-PEG-DSPE in liposomes, the cytotoxicity with KB cells was measured using a WST-8 assay. Doxorubicin concentrations leading to 50% cell death (IC_{50}) were determined from the concentration-dependent cell viability curves. As shown in Table 1, the IC_{50} value of 0.25F5-NL was the highest at 1.15 μg/mL. PEGylated liposomal doxorubicin, SL (IC_{50}, 3.37 μg/mL), showed lower toxicity than NL (IC_{50}, 2.39 μg/mL). However, modification of PEGylated liposomes by 0.25 mol% folate (0.25F5-SL) showed ~2.7 times higher toxicity (IC_{50}, 1.27 μg/mL) than SL, giving a similar level of cytotoxicity to folate-linked liposomes (0.25F5-NL). Free doxorubicin (IC_{50}, 0.65 μg/mL) showed much higher cytotoxicity than the liposomes. However, because free doxorubicin has a rapid systemic clearance rate, liposomes, especially with FR targeting, are likely to exhibit a therapeutic advantage over free doxorubicin *in vivo*.

The cellular uptake of folate-linked liposomes was increased by a longer PEG spacer and a higher density of F-PEG-DSPE. Such an increment corresponded well with enhanced cytotoxicity. Cellular association of SL was decreased because the mPEG layers inhibited interaction with cells, resulting in a cytotoxicity reduction. The major benefits of the mPEG layer exist only *in vivo*.

These results concerning folate-PEG spacer length in both NL and SL corresponded well with the previous report evaluated by cellular binding *in vitro*, in which the conjugation of folate to a shorter PEG spacer reduced folate exposure by interference with the ability of the liposome to recognize FR (8). With regard to folate density, maximal FR-dependent uptake of both NL and SL was obtained previously with a density of 0.2 to 0.5 mol% F-PEG-DSPE (10, 17, 28, 29). Our data on cellular uptake and *in vitro* cytotoxicity indicated that 0.25 mol% F5-PEG-DSPE in liposomes was optimal for targeting to FR on KB cells. It is known that the folate molecule can form dimers, trimers, and even self-assembling tubular quartets at higher concentrations (18). Similar to other glycosyl phosphatidylinositol-anchored proteins, FR molecules exist as clusters in specialized microdomains in the plasma membrane. Because FR can only bind one molecule of folic acid (19), such self-assembled multimers of folic acid are incapable of binding to FR. Therefore, an increase in the density of folate ligand on liposomes may not increase the level of binding to FR. The targeting efficiency of folate-linked vesicles was affected by the amount of folate-PEG lipid.

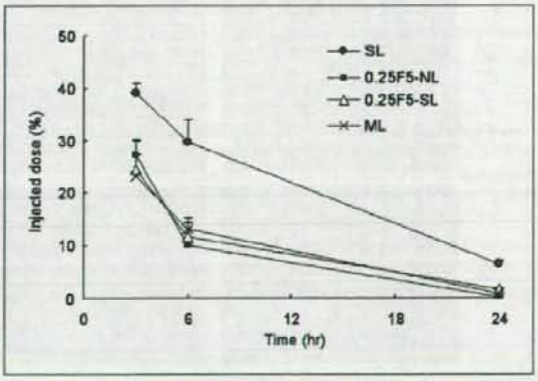

Fig. 3. Plasma concentration versus time curves of liposomal doxorubicin in mice. Liposomes were administered intravenous via tail vein injection at a dose of 5 mg/kg doxorubicin. The formulations used were SL (●), 0.25F5-SL (△), 0.25F5-NL (■), and ML (×). Mean ± SD (n = 3).

Table 2. Pharmacokinetic variables of liposomal doxorubicin in mice

Liposome	$AUC_{0-24\ h}$ (μg · h/mL)	Clearance (mL/h)
SL	491.2 ± 33.9**	0.3 ± 0.02
0.25F5-NL	190.2 ± 24.2**	0.7 ± 0.1
0.25F5-SL	212.1 ± 33.2**	0.6 ± 0.1
ML	218.0 ± 18.4**	0.6 ± 0.1

**, $P < 0.01$.

Serum doxorubicin level in mice after intravenous injection of folate-linked liposomal doxorubicin formulations. ML was designed to achieve a longer circulation time in the blood and also FR recognition on the tumor surface. The serum clearance kinetics of the various liposomal formulations in mice was compared as shown in Fig. 3 and Table 2. SL (AUC = 491.2 μg h/mL) exhibited a significantly longer circulation time than ML (AUC = 218.0 μg h/mL; clearance = 0.6 mL/h), 0.25F5-SL (AUC = 212.1 μg h/mL; clearance = 0.6 mL/h), and 0.25F5-NL (AUC = 190.2 μg h/mL; clearance = 0.7 mL/h; $P < 0.01$). Masking of the folate-linked liposomes, ML, did not achieve longer circulation times in the blood as well as 0.25F5-NL and 0.25F5-SL, as expected from the lower cellular uptake to KB cells. Our finding that 0.25F5-SL exhibited faster clearance than SL, corresponding with the previous study, indicated that the increase in folate modification of SL induced faster clearance than SL alone (9). This previous report indicated that this result was due to the distribution of folate-linked PEGylated liposomes over the internal organs, such as the liver, by the modification of folic acid (9). However, folate modification either inside or outside the mPEG-layer on the liposomes might lead to accumulation of liposomes in the tumor by FR targeting more significantly than the effect of longer circulation time. Next, we examined the distribution of folate-linked liposomal doxorubicin in tumors.

Distribution of folate-linked liposomal doxorubicin in M109 solid tumors. To evaluate the distribution of doxorubicin in

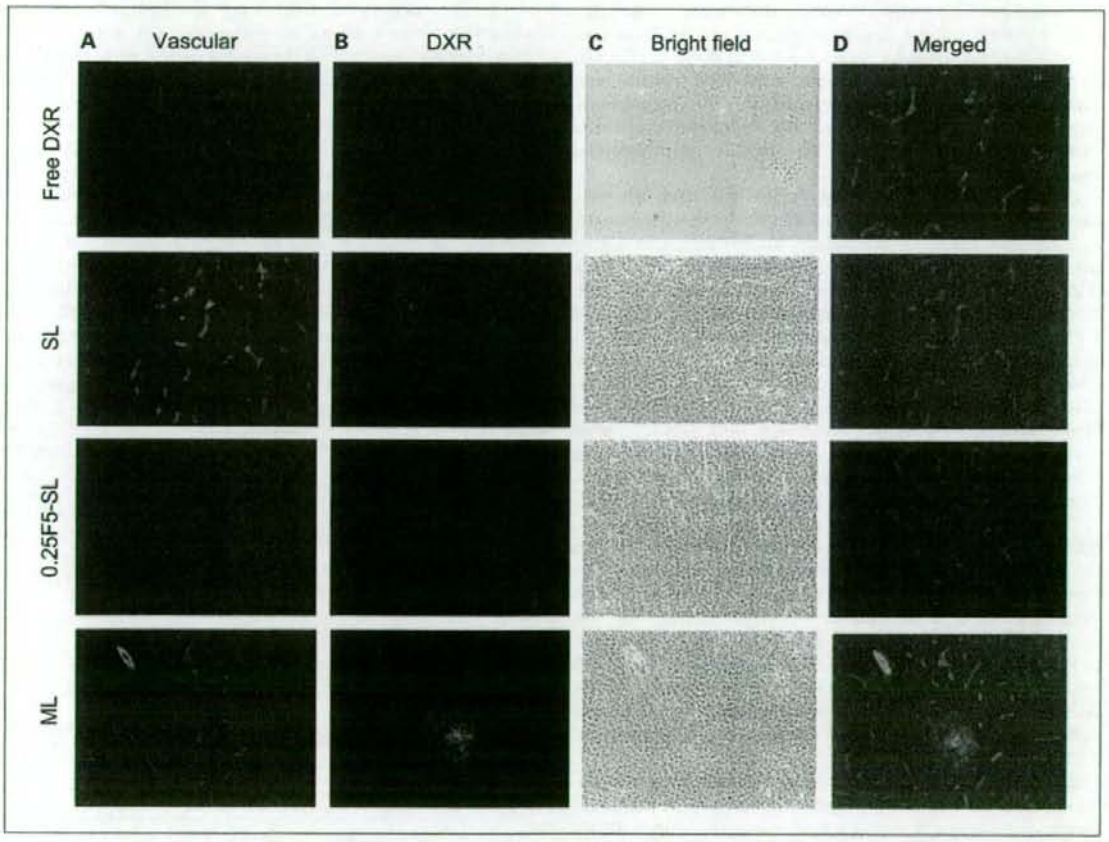

Fig. 4. Distribution of liposomal doxorubicin in M109 solid tumors measured by fluorescence microscopy. M109 cells were inoculated subcutaneously into female CDF1 mice. Twenty-four hours after intravenous administration of liposomes at a dose of 5 mg/kg doxorubicin, the tumor was excised and processed by frozen sectioning at 10 μm. Immunofluorescent staining of tumors by CD31 antibody is shown. Magnification, ×100. *Green signals*, location of neovessels; *red signals*, location of doxorubicin.

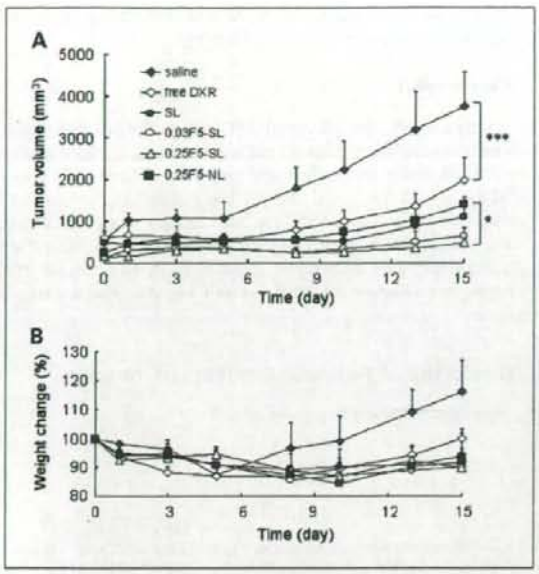

Fig. 5. Tumor growth inhibition by folate-linked liposomal doxorubicin in mice bearing M109 tumors. Tumor volume (*A*) and body weight change (*B*) after a single intravenous injection of liposomes at a dose of 10 mg/kg doxorubicin or with saline (♦). The formulations used were free doxorubicin (○), SL (●), 0.03 F5-SL (○), 0.25F5-SL (△), and 0.25F5-NL (■). ***, $P < 0.001$; *, $P < 0.05$. Mean ± SD ($n = 6$).

tumors after intravenous injection of liposome formulations, we observed the staining of neovessels with FITC-fluorescent CD31 antibodies using a fluorescence microscope (Fig. 4). Most of the red fluorescence due to free doxorubicin was not observed in tumors 24 h later, but doxorubicin was observed in other liposome formulations. Folate-linked liposomes, ML, tended to accumulate around blood vessels, although a big difference was not seen in comparison with SL and 0.25F5-SL. This finding indicated that folate-linked liposomal doxorubicin accumulated in the tumor, whereas it did not show long circulation as SL.

Antitumor effect of folate-linked liposomal doxorubicin evaluated in M109 solid tumors. Because the folate-linked liposomes of 0.25F5-NL and 0.25F5-SL showed higher cytotoxicity than nontargeted PEGylated liposomes (SL) *in vitro*, their antitumor effect was evaluated in mice bearing M109 cells, including 0.03F5-SL and ML. At first, each preparation of liposomes (SL, 0.03F5-SL, 0.25F5-SL, and 0.25F5-NL) and free doxorubicin solution were injected intravenously at doses of 10 mg/kg doxorubicin body weight.

As shown in Fig. 5A, the doxorubicin-injected group showed a high antitumor effect in comparison with saline-treated and free doxorubicin-treated groups. The antitumor effect of folate-linked PEGylated liposomes, 0.25F5-SL, was significantly higher than that of folate-linked non-PEGylated liposomes, 0.25F5-NL, on day 15 ($P < 0.05$).

Next as shown in Fig. 6A, the antitumor effect of free doxorubicin, 0.25F5-SL, 0.25F5-NL, and SL was compared with that of ML after intravenous injection at doses of 8 mg/kg doxorubicin body weight. ML showed similar effect with 0.25F5-SL, and both liposomes showed a significantly higher antitumor effect compared with 0.25F5-NL and free doxorubicin ($P < 0.01$) but not with SL ($P > 0.05$) on day 16. SL showed a significantly higher effect with 0.25F5-NL ($P < 0.05$).

Moreover, as a result of observation of side effects by administering doxorubicin, a tendency of weight loss was seen shortly after administering free doxorubicin but not for liposomal doxorubicin (Figs. 5 and 6B). In addition, conspicuous side effects such as diarrhea were not observed with liposomal doxorubicin.

The antitumor effect of folate-linked liposomal doxorubicin, ML, and 0.25F5-SL was not significantly higher than that of SL, which was not related to the accumulation of doxorubicin in blood vessels in the tumor region (as shown in Fig. 4). This phenomenon might be ascribed to the difference in drug release rate, which is regarded as an important factor influencing the biological activity of liposomal drugs (30, 31). In order for folate-linked liposomes to bind FR in a solid tumor via intravenous injection, they require extravasation from blood vessels in the tumor region, passage through the intercellular space, and finally reach FR on the tumor cell surface. Although folate-linked liposomal doxorubicin was retained in the tumor, release of the drug into the local environment might vary. After accumulation in the tumor, SL could effectively release the encapsulated drug and free

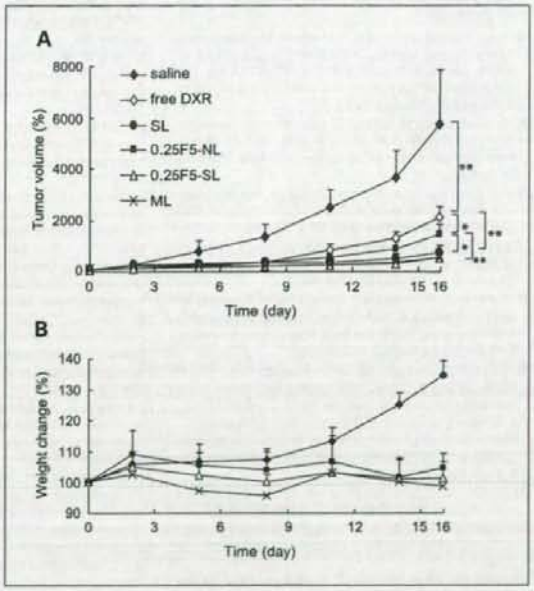

Fig. 6. Tumor growth inhibition by folate-linked and masked folate-linked liposomal doxorubicin in mice bearing M109 tumors. Tumor volume (*A*) and body weight change (*B*) after a single intravenous injection of liposomes at a dose of 8 mg/kg doxorubicin or with saline (♦). The formulations used were free doxorubicin (○), SL (●), 0.25F5-SL (△), 0.25F5-NL (■), and ML (×). Tumor volumes are plotted as ratios to their volume before the first drug injection. Mean ± SD ($n = 6$). **, $P < 0.01$; *, $P < 0.05$.

doxorubicin rapidly reached a therapeutic concentration that can inhibit tumor growth. In contrast, ML and 0.25F5-SL could accumulate relatively highly in the tumor but could not release the required amount of drug at an appropriate rate. In a nonsolid tumor, the high therapeutic efficacy of folate-linked liposomal doxorubicin was reported in mouse ascites leukemia models, in which the treatment route was intraperitoneal injection (14). In addition, the therapeutic efficacy of intravenous treatment with folate-linked liposomal doxorubicin was improved in mice inoculated intraperitoneally with lymphoma cells (32, 33). Therefore, further study is needed for FR targeting of solid tumors by intravenous injection of folate-linked liposomes. These findings suggested that, for active targeting using folate following intravenous injection, the sterically stabilized property of liposomes was needed as well as targeting to retard tumor growth, in contrast to the *in vitro* results. Folate-linked SLs and MLs with less circulation times showed comparative antitumor effect to traditional SL. Longer linker of folate and less PEG modification will allow the design of FR targeting liposome in the clinical setting.

Conclusion

In this study, the effects of PEG spacer length and ligand density on FR-targeted liposomes were evaluated. Folate ligands with 0.25 mol% and sufficiently long PEG spacers (F-PEG_{5000}-DSPE) of NLs increased the FR association and cytotoxicity compared with those of SLs and MLs *in vitro*. On the contrary, folate-linked SLs and MLs showed a higher tumor-killing effect than folate-linked NLs *in vivo*. Further study to optimize PEG coating for FR-targeting particles will improve the antitumor effect.

Disclosure of Potential Conflicts of Interest

No potential conflicts of interest were disclosed.

References

1. Weitman SD, Lark RH, Coney LR, et al. Distribution of the folate receptor GP38 in normal and malignant cell lines and tissue. Cancer Res 1992;52:3396–401.
2. Wu M, Gunning W, Ratnam M. Expression of folate receptor type α in relation to cell type, malignancy, and differentiation in ovary, uterus, and cervix. Cancer Epidemiol Biomarkers Prev 1999;8:775–82.
3. Elnakat H, Ratnam M. Distribution, functionality and gene regulation of folate receptor isoforms: implications in targeted therapy. Adv Drug Deliv Rev 2004; 56:1067–84.
4. Shen F, Ross JF, Wang X, Ratnam M. Identification of a novel folate receptor, a truncated receptor, and receptor type β in hematopoietic cells: cDNA cloning, expression, immunoreactivity, and tissue specificity. Biochemistry 1994;33:1209–15.
5. Ross JF, Wang H, Behm FG, et al. M. Folate receptor type β is a neutrophilic lineage marker and is differentially expressed in myeloid leukemia. Cancer 1999;85: 348–57.
6. Wang H, Ross JF, Ratnam M. Structure and regulation of a polymorphic gene encoding folate receptor type γ/γ'. Nucleic Acids Res 1998;26:2132–42.
7. Lee RJ, Low PS. Folate-mediated tumor cell targeting of liposome entrapped doxorubicin *in vitro*. Biochim Biophys Acta 1995;1233:134–44.
8. Gabizon A, Horowitz AT, Goren D, et al. Targeting folate receptor with folate linked to extremities of poly (ethylene glycol)-grafted liposomes: *in vitro* studies. Bioconjug Chem 1999;10:289–98.
9. Gabizon A, Horowitz AT, Goren D, et al. *In vivo* fate of folate-targeting polyethylene-glycol liposomes in tumor-bearing mice. Clin Cancer Res 2003;9:6551–9.
10. Goren D, Horowitz AT, Tzemach D, et al. Nuclear delivery of doxorubicin via folate-targeted liposomes with bypass of multidrug-resistance efflux pump. Clin Cancer Res 2000;6:1949–57.
11. Sudimack J, Lee RJ. Drug targeting via the folate receptor. Adv Drug Deliv Rev 2000;41:147–62.
12. Hofland HE, Masson C, Iginla S, et al. Folate-targeted gene transfer *in vivo*. Mol Ther 2002;5: 739–44.
13. Pan XQ, Zheng X, Shi G, et al. A strategy for the treatment of acute myelogenous leukemia based on folate receptor type-targeted liposomal doxorubicin combined with receptor induction using all-*trans*-retinoic acid. Blood 2002;100:594–602.
14. Pan XQ, Wang H, Lee RJ. Antitumor activity of folate receptor-targeted liposomal doxorubicin in a KB oral carcinoma murine xenograft model. Pharm Res 2003; 20:417–22.
15. Rait AS, Pirollo KF, Xiang L, Ulick D, Chang EH. Tumor-targeting, systemically delivered antisense HER-2 chemosensitizes human breast cancer xenografts irrespective of HER-2 levels. Mol Med 2002; 8:475–86.
16. Zhao X, Lee RJ. Tumor-selective targeted delivery of genes and antisense oligodeoxyribonucleotides via the folate receptor. Adv Drug Deliv Rev 2004;56: 1193–204.
17. Reddy JA, Abburi C, Hofland H, et al. Folate-targeted, cationic liposome-mediated gene transfer into disseminated peritoneal tumors. Gene Ther 2002;9: 1542–50.
18. Ciuchi F, Di Nicola G, Franz H, et al. Self-recognition and self-assembly of folic acid salts: columnar liquid crystalline polymorphism and the column growth process. J Am Chem Soc 1994;116:7064–71.
19. Antony AC, Utley C, Van Horne KC, Kolhouse JF. Isolation and characterization of a folate receptor from human placenta. J Biol Chem 1981;256:9684–92.
20. Shiokawa T, Hattori Y, Kawano K, et al. Effect of polyethylene glycol linker spacer length of folate-linked microemulsions loading aclacinomycin A on targeting ability and antitumor effect *in vitro* and *in vivo*. Clin Cancer Res 2005;11:2018–25.
21. Hayama A, Yamamoto T, Yokoyama M, et al. Polymeric micelles modified by folate-PEG-lipid for targeted drug delivery to cancer cells *in vitro*. J Nanosci Nanotech 2008;8:1–8.
22. Uster PS, Allen TM, Daniel BE, et al. Insertion of poly(ethylene glycol) derivatized phospholipid into pre-formed liposomes results in prolonged *in vivo* circulation time. FEBS Lett 1996;386:243–46.
23. Lee RJ, Wang S, Turk MJ, Low PS. The effects of pH and intraliposomal buffer strength on the rate of liposome content release and intracellular drug delivery. Biosci Rep 1998;18:69–78.
24. Matsushita Y, Iguchi H, Kiyosaki T, et al. A high performance liquid chromatographic method of analysis of 4'-*O*-tetrahydropyranyladriamycin and their metabolites in biological samples. J Antibiot (Tokyo) 1983; 36:880–6.
25. Takemoto S, Yamaoka K, Nishikawa M, Takakura Y. Histogram analysis of pharmacokinetic parameters by bootstrap resampling from one-point sampling data in animal experiments. Drug Metab Pharmacokinet 2006;21:458–64.
26. Li X, Hirsh DJ, Cabral-Lilly D, et al. Doxorubicin physical state in solution and inside liposomes loaded via a pH gradient. Biochim Biophys Acta 1998;1415: 23–40.
27. Paulos CM, Reddy JA, Leamon CP, et al. Ligand binding and kinetics of folate receptor recycling *in vivo*: impact on receptor-mediated drug delivery. Mol Pharmacol 2004;66:1406–14.
28. Saul JM, Annapragada A, Natarajan JV, Bellamkonda RV. Controlled targeting of liposomal doxorubicin via the folate receptor *in vitro*. J Control Release 2003;92:49–67.
29. Shmeeda H, Mak L, Tzemach D, et al. Intracellular uptake and intracavitary targeting of folate-conjugated liposomes in a mouse lymphoma model with up-regulated folate receptors. Mol Cancer Ther 2006;5: 818–24.
30. Cui J, Li C, Guo W, et al. Direct comparison of two pegylated liposomal doxorubicin formulations: is AUC predictive for toxicity and efficacy? J Control Release 2007;118:204–15.
31. Lim HJ, Masin D, Madden TD, Bally MB. Influence of drug release characteristics on the therapeutic activity of liposomal mitoxantrone. J Pharmacol Exp Ther 1997;281:566–73.
32. Gabizon A, Shmeeda H, Horowitz AT, Zalipsky S. Tumor cell targeting of liposome-entrapped drugs with phospholipid-anchored folic acid-PEG conjugates. Adv Drug Deliv Rev 2004;56:1177–92.
33. Shmeeda H, Mak L, Tzemach D, Astrahan P, Tarshish M, Gabizon A. Intracellular uptake and intracavitary targeting of folate-conjugated liposomes in a mouse lymphoma model with up-regulated folate receptors. Mol Cancer Ther 2006;5:818–24.

Int. J. Cancer: **122**, 2148–2153 (2008)

Synergistic antitumor activity of the novel SN-38-incorporating polymeric micelles, NK012, combined with 5-fluorouracil in a mouse model of colorectal cancer, as compared with that of irinotecan plus 5-fluorouracil

Takako Eguchi Nakajima[1,2], Masahiro Yasunaga[2], Yasuhiko Kano[3], Fumiaki Koizumi[4], Ken Kato[1], Tetsuya Hamaguchi[1], Yasuhide Yamada[1], Kuniaki Shirao[1], Yasuhiro Shimada[1] and Yasuhiro Matsumura[2]*

[1]*Gastrointestinal Oncology Division, National Cancer Center Hospital, Tokyo, Japan*
[2]*Investigative Treatment Division, Research Center for Innovative Oncology, National Cancer Center Hospital East, Kashiwa, Chiba, Japan*
[3]*Hematology Oncology, Tochigi Cancer Center, Tochigi, Japan*
[4]*Shien Lab Medical Oncology Division, National Cancer Center Hospital, Tokyo, Japan*

The authors reported in a previous study that NK012, a 7-ethyl-10-hydroxy-camptothecin (SN-38)-releasing nano-system, exhibited high antitumor activity against human colorectal cancer xenografts. This study was conducted to investigate the advantages of NK012 over irinotecan hydrochloride (CPT-11) administered in combination with 5-fluorouracil (5FU). The cytotoxic effects of NK012 or SN-38 (an active metabolite of CPT-11) administered in combination with 5FU was evaluated *in vitro* in the human colorectal cancer cell line HT-29 by the combination index method. The effects of the same drug combinations was also evaluated *in vivo* using mice bearing HT-29 and HCT-116 cells. All the drugs were administered i.v. 3 times a week; NK012 (10 mg/kg) or CPT11 (50 mg/kg) was given 24 hr before 5FU (50 mg/kg). Cell cycle analysis in the HT-29 tumors administered NK012 or CPT-11 *in vivo* was performed by flow cytometry. NK012 exerted more synergistic activity with 5FU compared to SN-38. The therapeutic effect of NK012/5FU was significantly superior to that of CPT-11/5FU against HT-29 tumors ($p = 0.0004$), whereas no significant difference in the antitumor effect against HCT-116 tumors was observed between the 2-drug combinations ($p = 0.2230$). Cell-cycle analysis showed that both NK012 and CPT-11 tend to cause accumulation of cells in the S phase, although this effect was more pronounced and maintained for a more prolonged period with NK012 than with CPT-11. Optimal therapeutic synergy was observed between NK012 and 5FU, therefore, this regimen is considered to hold promise of clinical benefit, especially for patients with colorectal cancer.
© *2008 Wiley-Liss, Inc.*

Key words: NK012; SN-38; 5-fluorouracil; drug delivery system; colorectal cancer

The 5-year survival rates of colorectal cancer (CRC) have improved remarkably over the last 10 years, accounted for in large part by the extensively investigated agents after 5-fluorouracil (5FU). Irinoetcan hydrochloride (CPT-11), a water-soluble, semi-synthetic derivative of camptothecin, is one such agent that has been shown to be highly effective, and currently represents a key-drug in first- and second-line treatment regimens for CRC. CPT-11 monotherapy, however, has not been shown to yield superior efficacy, including in terms of the median survival time, to bolus 5FU/leucovorin (LV) alone.[1] In 2 Phase III trials, the addition of CPT-11 to bolus or infusional 5FU/LV regimens clearly yielded greater efficacy than administration of 5FU/LV alone, with a doubling of the tumor response rate and prolongation of the median survival time by 2–3 months.[1,2]

CPT-11 is converted to 7-ethyl-10-hydroxy-camptothecin (SN-38), a biologically active and water-insoluble metabolite of CPT-11, by carboxylesterases in the liver and the tumor. SN-38 has been demonstrated to exhibit up to a 1,000-fold more potent cytotoxic activity than CPT-11 against various cancer cells *in vitro*.[3] The metabolic conversion rate is, however, very low, with only <10% of the original volume of CPT-11 being metabolized to SN-38[4,5]; conversion of CPT-11 to SN-38 also depends on genetic interindividual variability of the activity of carboxylesterases.[6] Direct use of SN-38 itself for clinical cancer treatment must be shown to be identical in terms of both efficacy and toxicity.

Some drugs incorporated in drug delivery systems (DDS), such as Abraxane and Doxil, are already in clinical use.[7,8] The clinical benefits of DDS are based on their EPR effect.[9] The EPR effect is based on the pathophysiological characteristics of solid tumor tissues: hypervascularity, incomplete vascular architecture, secretion of vascular permeability factors stimulating extravasation within cancer tissue, and absence of effective lymphatic drainage from the tumors that impedes the efficient clearance of macromolecules accumulated in solid tumor tissues. Several types of DDS can be used for incorporation of a drug. A liposome-based formulation of SN-38 (LE-SN38) has been developed, and a clinical trial to assess its efficacy is now under way.[10,11]

Recently, we demonstrated that NK012, novel SN-38-incorporating polymeric micelles, exerted superior antitumor activity and less toxicity than CPT-11.[12] NK012 is characterized by a smaller size of the particles than LE-SN38; the mean particle diameter of NK012 is 20 nm. NK012 can release SN-38 under neutral conditions even in the absence of a hydrolytic enzyme, because the bond between SN-38 and the block copolymer is a phenol ester bond, which is stable under acidic conditions and labile under mild alkaline conditions. The release rate of SN-38 from NK012 under physiological conditions is quite high; more than 70% of SN-38 is released within 48 hr. We speculated that the use of NK012, in place of CPT-11, in combination with 5FU may yield superior results in the treatment of CRC. In the present study, we evaluated the antitumor activity of NK012 administered in combination with 5FU as compared to that of CPT-11 administered in combination with 5FU against CRC in an experimental model.

Material and methods

Cells and animals

The human colorectal cancer cell lines used, namely, HT-29 and HCT-116, were purchased from the American Type Culture Collection (Rockville, MD). The HT-29 cells and HCT-116 cells were maintained in RPMI 1640 supplemented with 10% fetal bovine serum (Cell Culture Technologies, Gaggenau-Hoerden, Germany), penicillin, streptomycin, and amphotericin B (100 units/mL, 100 μg/mL, and 25 μg/mL, respectively; Sigma. St. Louis, MO) in a humidified atmosphere containing 5% CO_2 at 37°C.

BALB/c *nu/nu* mice were purchased from SLC Japan (Shizuoka, Japan). Six-week-old mice were subcutaneously (s.c.)

***Correspondence to:** Investigative Treatment Division, Research Center for Innovative Oncology, National Cancer Center Hospital East, 6-5-1 Kashiwanoha, Kashiwa, Chiba 277-8577, Japan. Fax: +81-4-7134-6866. E-mail: yhmatsum@east.ncc.go.jp
Received 2 September 2007; Accepted after revision 20 November 2007
DOI 10.1002/ijc.23381
Published online 14 January 2008 in Wiley InterScience (www.interscience.wiley.com).

inoculated with 1×10^6 cells of HT-29 or HCT-116 cell line in the flank region. The length (a) and width (b) of the tumor masses were measured twice a week, and the tumor volume (TV) was calculated as follows: $TV = (a \times b^2)/2$. All animal procedures were performed in compliance with the Guidelines for the Care and Use of Experimental Animals established by the Committee for Animal Experimentation of the National Cancer Center; these guidelines meet the ethical standards required by law and also comply with the guidelines for the use of experimental animals in Japan.

Drugs

The SN-38-incorporating polymeric micelles, NK012, and SN-38 were prepared by Nippon Kayaku (Tokyo, Japan).[12] CPT-11 was purchased from Yakult Honsha (Tokyo, Japan). 5FU was purchased from Kyowa Hakko (Tokyo, Japan).

Cell growth inhibition assay

HT-29 cells were seeded in 96-well plates at a density of 2,000 cells/well in a final volume of 90 μL. Twenty-four hours after seeding, a graded concentration of NK012 or SN-38 was added concurrently with 5FU to the culture medium of the HT-29 cells in a final volume of 100 μL for drug interaction studies. The culture was maintained in the CO_2 incubator for an additional 72 hr. Then, cell growth inhibition was measured by the tetrazolium salt-based proliferation assay (WST assay; Wako Chemicals, Osaka, Japan). WST-1 labeling solution (10 μL) was added to each well and the plates were incubated at 37°C for 3 hr. The absorbance of the formazan product formed was detected at 450 nm in a 96-well spectrophotometric plate reader. Cell viability was measured and compared to that of the control cells. Each experiment was carried out in triplicate and was repeated at least 3 times. Data were averaged and normalized against the nontreated controls to generate dose-response curves.

Drug interaction analysis

The nature of interaction between NK012 or SN-38 and 5FU against HT-29 cells was evaluated by median-effect plot analyses and the combination index (CI) method of Chou and Talalay.[13] Data analysis was performed using the Calcusyn software (Biosoft, NY, USA). NK012 or SN-38 was combined with 5FU at a fixed ratio that spanned the individual IC_{50} values of each drug. The IC_{50} values were determined on the basis of the dose-response curves using the WST assay. For any given drug combination, the CI is known to represent the degree of synergy, additivity or antagonism. It is expressed in terms of fraction-affected (Fa) values, which represents the percentage of cells killed or inhibited by the drug. Isobologram equations and Fa/CI plots were constructed by computer analysis of the data generated from the median effect analysis. Each experiment was performed in triplicate with 6 gradations and was repeated at least 3 times. The resultant dose-response curves were averaged, to create a single composite dose-response curve for each combination.

In vivo analysis of the effects of NK012 combined with 5FU as compared to those of CPT-11 combined with 5FU

When the mean tumor volumes reached ~93 mm^3, the mice were randomly divided into test groups consisting of 5 mice per group (Day 0). The drugs were administered i.v. *via* the tail vein of the mice. In the groups administered NK012 or 5FU as single agents, the drug was administered on Days 0, 7 and 14. In the combined treatment groups, NK012 or CPT-11 was administered 24 hr before 5FU on Days 0, 7 and 14, according to the previously reported combination schedule for CPT-11 and 5FU.[14] Complete response (CR) was defined as tumor not detectable by palpation at 90 days after the start of treatment, at which time-point the mice were sacrificed. Tumor volume and body weight were measured twice a week. As a general rule, animals in which the tumor volume exceeded 2,000 mm^3 were also sacrificed.

Experiment 1. Evaluation of the effects of NK012 combined with 5FU and determination of the maximum tolerated dose (MTD) of NK012/5FU. By comparing the data between NK012 administered as a single agent and NK012/5FU, we evaluated the effects of the combined regimen against the s.c HT-29 tumors. A preliminary experiment showed that combined administration of NK012 15 mg/kg + 5FU 50 mg/kg every 6 days caused drug-related lethality (data not shown). To determine the MTD, therefore, we set the dosing schedule of the combined regimen at 5 or 10 mg/kg of NK012 + 50 mg/kg of 5FU three times a week.

Experiment 2. Comparison of the antitumor effect of NK012/5FU and CPT-11/5FU. Based on a comparison of the data between NK012/5FU and CPT-11/5FU against the s.c. HT-29 and HCT-116 tumors, we investigated the feasibility of the clinical application of NK012/5FU for the treatment of CRC. CPT-11/5FU was administered three times a week at the respective MTDs of the 2 drugs as previously reported, that is, CPT11 at 50 mg/kg and 5FU at 50 mg/kg, respectively.[14] NK012/5FU was administered once three times a week at the respective MTDs of the 2 drugs determined from Experiment 1.

Cell cycle analysis

Samples from the HT-29 tumors that had grown to 80–100 mm^3 were removed from the mice at 6, 24, 48, 72 and 96 hr after the administration of NK012 alone at 10 mg/kg or CPT-11 alone at 50 mg/kg. The samples were excised, minced in PBS and fixed in 70% ethanol at −20°C for 48 hr. They were then digested with 0.04% pepsin (Sigma chemical Co., St Lous, MO) in 0.1 N HCL for 60 min at 37°C in a shaking bath to prepare single-nuclei suspensions. The nuclei were then centrifuged, washed twice with PBS and stained with 40 μg/mL of propidium iodide (Molecular Probes, OR) in the presence of 100 μg/mL RNase in 1 mL PBS for 30 min at 37°C. The stained nuclei were analyzed with B-D FACSCalibur (BD Biosciences, San Jose, CA), and the cell cycle distribution was analyzed using the Modfit program (Verity Software House Topsham, ME).

Statistical analyses

Data were expressed as mean ± SD. Data were analysed with Student's t test when the groups showed equal variances (F test), or Welch's test when they showed unequal variances (F test). $p < 0.05$ was regarded as statistically significant. All statistical tests were 2-sided.

Results

Antiproliferative effects of NK012 or SN-38 administered in combination with 5FU

Figure 1*a* shows the dose-response curves for NK012 alone, 5FU alone and a combination of the two. The IC_{50} levels of NK012 and 5FU against the HT-29 cells were 39 nM and 1 μM, respectively, and the IC_{50} level of SN-38 was 14 nM (data not shown). Based on these data, the molar ratio of NK012 or SN-38:5FU of 1:1,000 was used for the drug combination studies.

Figures 1*b* and 1*c* show the median-effect and the combination index plots. Combination indices (CIs) of <1.0 are indicative of synergistic interactions between 2 agents; additive interactions are indicated by CIs of 1.0, and antagonism by CIs of >1.0. Figure 1*c* shows the combination index for NK012 and 5FU, when 2 drugs are supposed to be mutually exclusive. Marked synergism was observed between Fa 0.2 and 0.6. Theoretically, the CI method is the most reliable around an Fa of 0.5, suggesting synergistic effects of the combination of NK012 and 5FU. This synergistic effect was more evident than that of SN-38/5FU (Fig. 1*d*).

In vivo *effect of combined NK012 and 5FU*

Experiment 1. Dose optimization and effect of combined NK012 and 5FU against HT-29 tumors. Comparison of the relative tumor volumes on Day 40 revealed significant differences between

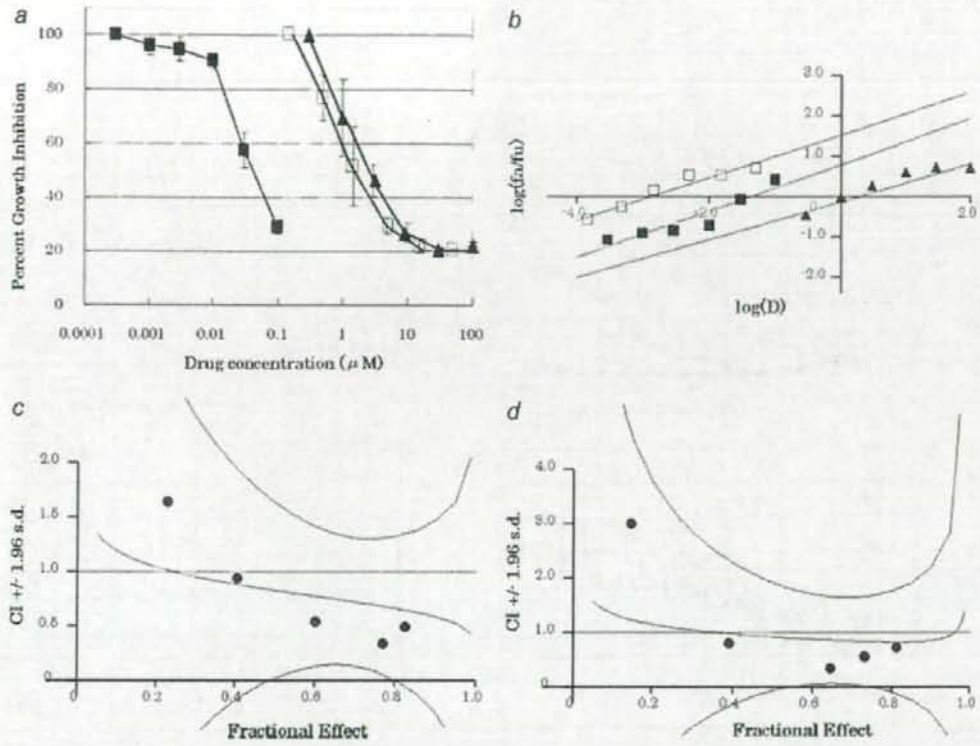

FIGURE 1 – Interaction of NK012 and 5FU *in vitro*. (*a*) Dose-response curves for NK012 alone (■), 5FU alone (▲) and their combination (□) against HT-29 cells. HT-29 cells were seeded at 2,000 cells/well. Twenty-four hours after seeding, a graded concentration of NK012 or 5FU was added to the culture medium of the HT-29 cells. Cell growth inhibition was measured by WST assay after 72 hr of treatment. Cell viability was measured and compared with that of the control cells. Each experiment was carried out independently and repeated at least 3 times. Points, mean of tripricates; bars, SD. (*b*) Median effect plot for the interaction of NK012 and 5FU. (*c*, *d*) Combination index for the interaction as a function of the level of effect (fraction effect = 0.5 is the IC_{50}). The straight line across the CI value of 1.0 indicates additive effect and CIs above and below indicate antagonism and synergism, respectively. The molar ratio of NK012/5FU (*c*) or SN-38/5FU (*d*) at 1:1,000 was tested by CI analysis. Black circles represent the CIs of the actual data points, solid lines represent the computer-derived CIs at effect levels ranging from 10 to 100% inhibition of cell growth, and the dotted lines represent the 95% confidence intervals.

those in the mice administered NK012 alone and those administered NK012/5FU at 5 mg/kg of NK012 ($p = 0.018$) (Fig. 2*a*). Although there was no statistically significant difference in the relative tumor volume measured on Day 54 between the mice administered NK012 alone and NK012/5FU at 10 mg/kg of NK012 ($p = 0.3050$), a trend of superior antitumor effect was demonstrated in the group treated with NK012/5FU at 10 mg/kg of NK012 (Fig. 2*a*). The CR rates were 20, 40 and 60% for 5 mg/kg NK012 + 50 mg/kg 5FU, 10 mg/kg NK012 alone and 10 mg/kg NK012 + 50 mg/kg 5FU, respectively. The schedule of 10 mg/kg NK012 + 50 mg/kg 5FU resulted in no remarkable toxicity in terms of body weight changes, and these doses were determined as representing the MTDs (Fig. 2*b*).

Experiment 2. Comparison of the antitumor effect of combined NK012/5FU and CPT-11/5FU against HT-29 and HCT-116 tumors. The therapeutic effect of NK012/5FU on Day 60 was significantly superior to that of CPT-11/5FU against the HT-29 tumors ($p = 0.0004$) (Fig. 3*a*). A more potent antitumor effect, namely, a 100% CR rate, was obtained in the NK012/5FU group as compared to the 0% CR rate in the CPT-11/5FU group. Although no statistically significant difference in the relative tumor volume on Day 61 was demonstrated between the NK012/5FU and CPT-11/5FU in the case of the HCT-116 tumors ($p = 0.2230$), a trend of superior antitumor effect against these tumors was observed in the NK012/5FU treatment group (Fig. 3*b*). The CR rates for the case of the HCT-116 tumors were 0% in both NK012/5FU and CPT-11/5FU groups.

Specificity of cell cycle perturbation

We studied the differences in the effects between NK012 10 mg/kg and CPT-11 50 mg/kg on the cell cycle (Fig. 4*a*). The data indicated that both NK012 and CPT-11 tended to cause accumulation of cells in the S phase, although the effect of NK012 was stronger and maintained for a more prolonged period than that of CPT-11; the maximal percentage of S-phase cells in the total cell population in the tumors was 34% at 24 hr after the administration of CPT-11, whereas it was 39% at 48 hr after the administration of NK012 (Figs. 4*b*, and 4*c*).

Discussion

Our primary endpoint was to clarify the advantages of NK012 over CPT-11 administered in combination with 5FU. We demonstrated that combined NK012 and 5FU chemotherapy exerts more

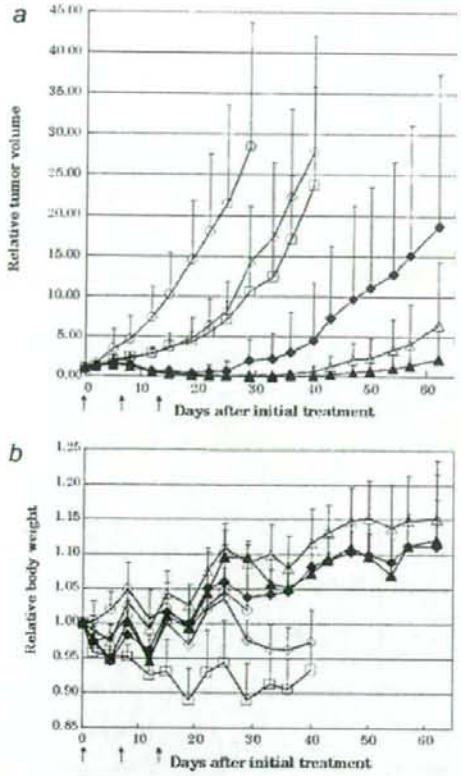

FIGURE 2 – Effect of NK012 alone or NK012 in combination with 5FU against HT-29 tumor-bearing mice. Points, mean; bars, SD. (*a*) Antitumor effect of each regimen on Days 0, 7 and 14. (○) control, (□) 5FU 50 mg/kg alone, (◇) NK012 5 mg/kg alone, (◆) NK012 5 mg/kg 24 hr before 5FU 50 mg/kg, (△) NK012 10 mg/kg alone, (▲) NK012 10 mg/kg 24 hr before 5FU 50 mg/kg. (*b*) Changes in the relative body weight. Data were derived from the same mice as those used in the present study.

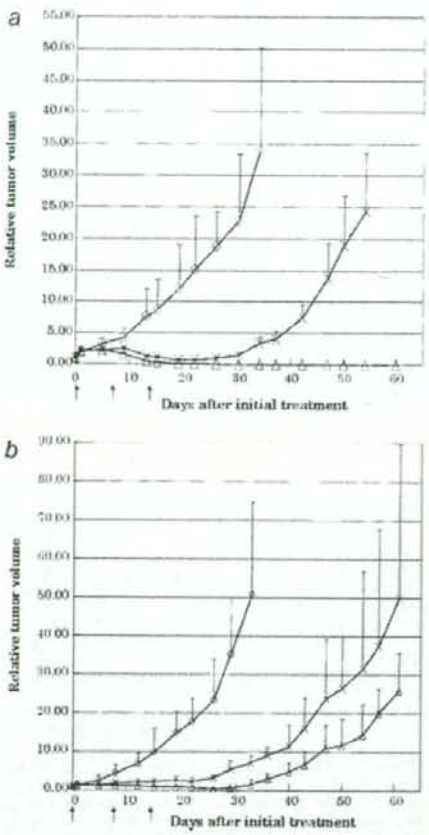

FIGURE 3 – Effect of NK012/5FU as compared with that of CPT11/5FU against HT-29 (*a*) or HCT-116 (*b*) tumor-bearing mice. Antitumor effect of each schedule on Days 0, 7 and 14. (○) control, (×) CPT-11 50 mg/kg 24 hr before 5FU 50 mg/kg, (△) NK012 10 mg/kg 24 hr before 5FU 50 mg/kg. Points, mean; bars, SD.

synergistic activity *in vitro* and significantly greater antitumor activity against human CRC xenografts as compared to CPT-11/5FU. The combination of NK012 and 5FU is considered to hold promise of clinical benefit for patients with CRC.

CPT-11, a topoisomerase-I inhibitor, and 5FU, a thymidilate synthase inhibitor, have been demonstrated to be effective agents for the treatment of CRC. A combination of these 2 drugs has also been demonstrated to be clearly more effective than either CPT-11 or 5FU/LV administered alone *in vivo* and in clinical settings.[1,2,14] Administration of 5FU by infusion with CPT-11 was shown to be associated with reduced toxicity and an apparent improvement in survival as compared to that of administration of the drug by bolus injection with CPT-11.[1,2] This synergistic enhancement may result from the mechanism of action of the 2 drugs; CPT-11 has been reported to cause accumulation of cells in the S phase, and 5FU infusion is known to cause DNA damage specifically in cells of the S phase.[14] On the basis of this background, our results suggesting the more pronounced and more prolonged accumulation of the tumor cells in the S phase caused by NK012 as compared with that by CPT-11 may explain the more effective synergy of the former administered with 5FU infusion. This may be attributable to accumulation of NK012 due to the enhanced permeability and retention (EPR) effect.[9] It is also speculated that NK012 allows sustained release of free SN-38, which may move more freely in the tumor interstitium.[15] Otherwise NK012 itself could internalize into cells to localize in several cytoplasmic organelles as reported by Savic *et al.*[16] These characteristics of NK012 may be responsible for its more potent antitumor activity observed in this study, because CPT-11 has been reported to show time-dependent growth-inhibitory activity against the tumor cells.[17]

The major dose-limiting toxicities of CPT-11 are diarrhea and neutropenia. SN-38, the active metabolite of CPT-11, may cause CPT-11-related diarrhea as a result of mitotic -inhibitory activity.[18] Because it undergoes significant biliary excretion, SN-38 may have a potentially long residence time in the gastrointestinal tract that may be associated with prolonged diarrhea.[19,20] In our previous report, we evaluated the tissue distribution of SN-38 after administration of an equimolar amount of NK012 (20 mg/kg) and CPT-11 (30 mg/kg), and found no difference in the level of SN-38 accumulation in the small intestine.[12] A significant antitumor effect of NK012 with a lower incidence of diarrhea was also dem-

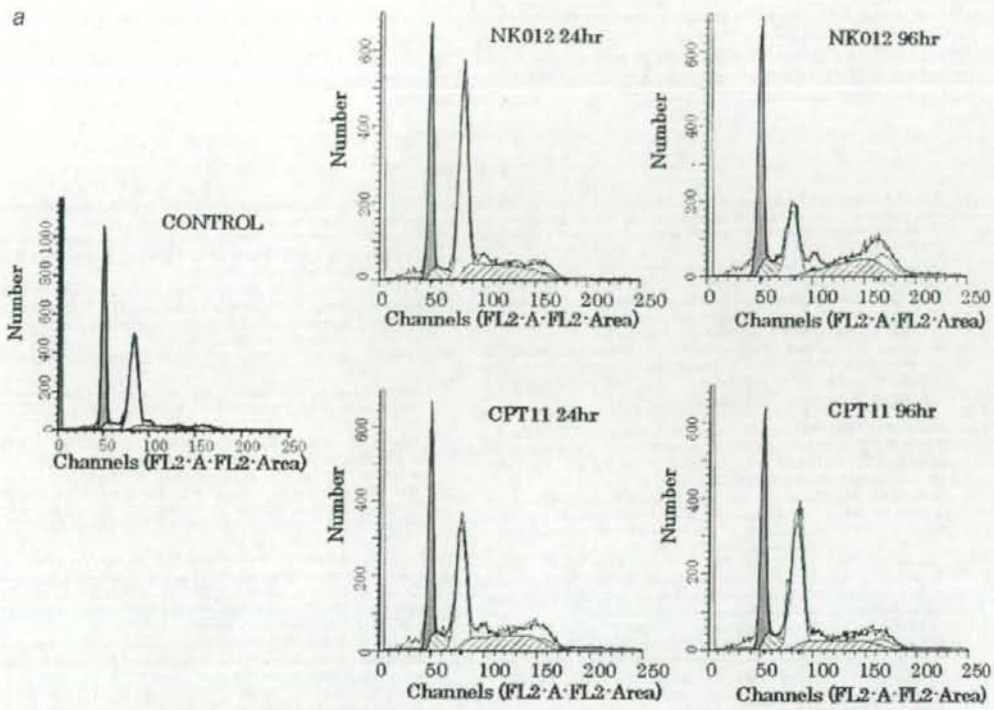

FIGURE 4 – Cell cycle analysis of HT-29 tumor cells collected 24, 48, 72 and 96 hr after administration of NK012 at 10 mg/kg alone or CPT-11 at 50 mg/kg alone using the Modfit program (Verity Software House Topsham, ME). (*a*) Cell cycle analysis of HT-29 tumor cells 24 and 96 hr after administration of NK012 at 10 mg/kg or CPT-11 at 50 mg/kg, respectively. (*b*) Cell cycle distribution of tumor cells 0, 24, 48, 72 and 96 hr after treatment with NK012 at 10 mg/kg. (*c*) Cell cycle distribution of tumor cells 0, 24, 48, 72 and 96 hr after treatment with CPT-11 at 50 mg/kg.

onstrated as compared to that observed with CPT-11 in a rat mammary tumor model.[21] Combined administration of CPT-11 with 5FU/LV infusion appears to be associated with acceptable toxicity in patients with CRC. In addition, no significant difference in the frequency of Grade 3/4 diarrhea was noted between patients treated with FOLFIRI (CPT-11 regimen with bolus and infusional 5FU/LV) and those treated with FOLFOX6 (oxaliplatin regimen with bolus and infusional 5FU/LV).[22,23] Our *in vivo* data actually revealed no severe body weight loss in the NK012/5FU group. Consequently, we expect that the NK012/5FU regimen, especially

with infusional 5FU, may be an attractive arm for a Phase III trial in CRC, with CPT-11/5FU as the control arm. We have already initiated a Phase I trial of NK012 in patients with advanced solid tumors based on the data suggesting higher efficacy and lower toxicity of this preparation than CPT-11 *in vivo*.[12]

In conclusion, we demonstrated that combined NK012 and 5FU chemotherapy exerts significantly greater antitumor activity against human CRC xenografts as compared to CPT-11/5FU, indicating the necessity of clinical evaluation of this combined regimen.

References

1. Saltz LB, Douillard JY, Pirotta N, Alakl M, Gruia G, Awad L, Elfring GL, Locker PK, Miller LL. Irinotecan plus fluorouracil/leucovorin for metastatic colorectal cancer: a new survival standard. Oncologist 2001;6:81–91.
2. Douillard JY, Cunningham D, Roth AD, Navarro M, James RD, Karasek P, Jandik P, Iveson T, Carmichael J, Alakl M, Gruia G, Awad L, et al. Irinotecan combined with fluorouracil compared with fluorouracil alone as first-line treatment for metastatic colorectal cancer: a multicentre randomised trial. Lancet 2000;355:1041–7.
3. Takimoto CH, Arbuck SG. Topoisomerase I targeting agents: the camptothecins. In: Chabner BA, Lango DL, eds. Cancer chemotherapy and biotherapy: principal and practice, 3rd ed. Philadelphia, PA: Lippincott Williams and Wilkins, 2001. 579–646.
4. Slatter JG, Schaaf LJ, Sams JP, Feenstra KL, Johnson MG, Bombardt PA, Cathcart KS, Verburg MT, Pearson LK, Compton LD, Miller LL, Baker DS, et al. Pharmacokinetics, metabolism, and excretion of irinotecan (CPT-11) following I.V. infusion of [(14)C]CPT-11 in cancer patients. Drug Metab Dispos 2000;28:423–33.
5. Rothenberg ML, Kuhn JG, Burris HA, III, Nelson J, Eckardt JR, Tristan-Morales M, Hilsenbeck SG, Weiss GR, Smith LS, Rodriguez GI, Rock MK, Von Hoff DD. Phase I and pharmacokinetic trial of weekly CPT-11. J Clin Oncol 1993;11:2194–204.
6. Guichard S, Terret C, Hennebelle I, Lochon I, Chevreau P, Fretigny E, Selves J, Chatelut E, Bugat R, Canal P. CPT-11 converting carboxylesterase and topoisomerase activities in tumour and normal colon and liver tissues. Br J Cancer 1999;80:364–70.
7. Gradishar WJ, Tjulandin S, Davidson N, Shaw H, Desai N, Bhar P, Hawkins M, O'Shaughnessy J. Phase III trial of nanoparticle albumin-bound paclitaxel compared with polyethylated castor oil-based paclitaxel in women with breast cancer. J Clin Oncol 2005;23:7794–803.
8. Muggia FM. Liposomal encapsulated anthracyclines: new therapeutic horizons. Curr Oncol Rep 2001;3:156–62.
9. Matsumura Y, Maeda H. A new concept for macromolecular therapeutics in cancer chemotherapy: mechanism of tumoritropic accumulation of proteins and the antitumor agent smancs. Cancer Res 1986;46:6387–92.
10. Zhang JA, Xuan T, Parmar M, Ma L, Ugwu S, Ali S, Ahmad I. Development and characterization of a novel liposome-based formulation of SN-38. Int J Pharm 2004;270:93–107.
11. Kraut EH, Fishman MN, LoRusso PM, Gorden MS, Rubin EH, Haas A, Fetterly GJ, Cullinan P, Dul JL, Steinberg JL. Final result of a phase I study of liposome encapsulated SN-38 (LE-SN38): safety, pharmacogenomics, pharmacokinetics, and tumor response [abstract 2017]. Proc Am Soc Clin Oncol 2005;23:139S.
12. Koizumi F, Kitagawa M, Negishi T, Onda T, Matsumoto S, Hamaguchi T, Matsumura Y. Novel SN-38-incorporating polymeric micelles, NK012, eradicate vascular endothelial growth factor-secreting bulky tumors. Cancer Res 2006;66:10048–56.
13. Chou TC, Talalay P. Quantitative analysis of dose-effect relationships: the combined effects of multiple drugs or enzyme inhibitors. Adv Enzyme Regul 1984;22:27–55.
14. Azrak RG, Cao S, Slocum HK, Toth K, Durrani FA, Yin MB, Pendyala L, Zhang W, McLeod HL, Rustum YM. Therapeutic synergy between irinotecan and 5-fluorouracil against human tumor xenografts. Clin Cancer Res 2004;10:1121–9.
15. Jain RK. Barriers to drug delivery in solid tumors. Sci Am 1994; 271:58–65.
16. Savic R, Luo L, Eisenberg A, Maysinger D. Micellar nanocontainers distribute to defined cytoplasmic organelles. Science 2003;300:615–18.
17. Kawato Y, Aonuma M, Hirota Y, Kuga H, Sato K. Intracellular roles of SN-38, a metabolite of the camptothecin derivative CPT-11, in the antitumor effect of CPT-11. Cancer Res 1991;51:4187–91.
18. Slater R, Radstone D, Matthews L, McDaid J, Majeed A. Hepatic resection for colorectal liver metastasis after downstaging with irinotecan improves survival. Proc Am Soc Clin Oncol 2003;22(abstract 1287).
19. Araki E, Ishikawa M, Iigo M, Koide T, Itabashi M, Hoshi A. Relationship between development of diarrhea and the concentration of SN-38, an active metabolite of CPT-11, in the intestine and the blood plasma of athymic mice following intraperitoneal administration of CPT-11. Jpn J Cancer Res 1993;84:697–702.
20. Atsumi R, Suzuki W, Hakusui H. Identification of the metabolites of irinotecan, a new derivative of camptothecin, in rat bile and its biliary excretion. Xenobiotica 1991;21:1159–69.
21. Onda T, Nakamura I, Seno C, Matsumoto S, Kitagawa M, Okamoto K, Nishikawa K, Suzuki M. Superior antitumor activity of NK012, 7-ethyl-10-hydroxycamptoyhecin-incorporating micellar nanoparticle, to irinotecan. Proc Am Assoc Cancer Res 2006;47:720s(abstract 3062).
22. Tournigand C, Andre T, Achille E, Lledo G, Flesh M, Mery-Mignard D, Quinaux E, Couteau C, Buyse M, Ganem G, Landi B, Colin P, et al. FOLFIRI followed by FOLFOX6 or the reverse sequence in advanced colorectal cancer: a randomized GERCOR study. J Clin Oncol 2004;22:229–37.
23. Colucci G, Gebbia V, Paoletti G, Giuliani F, Caruso M, Gebbia N, Carteni G, Agostara B, Pezzella G, Manzione L, Borsellino N, Misino A, et al. Phase III randomized trial of FOLFIRI versus FOLFOX4 in the treatment of advanced colorectal cancer: a multicenter study of the Gruppo Oncologico Dell'Italia Meridionale. J Clin Oncol 2005; 23:4866–75.